TFA

ACTA FACULTATIS TECHNICAE

TECHNICAL UNIVERSITY IN ZVOLEN

2

ISSUE: XXVII
ZVOLEN 2022

TABLE OF CONTENTS

SCIENTIFIC PAPERS

SCIENTIFIC PAPERS

EFFECTIVE USE OF THE LASER PARTICLE DETECTOR IN FAULT DIAGNOSTICS OF HYDRAULIC SYSTEMS

EFEKTÍVNE VYUŽITIE LASEROVÉHO DETEKTORA ČASTÍC PRI PORUCHOVEJ DIAGNOSTIKE HYDRAULICKÝCH SYSTÉMOV

Jakub Drmla[1]

[1]*Katedra mechaniky, strojníctva a dizajnu, Fakulta techniky, Technická univerzita vo Zvolene, Študentská 26, 960 53 Zvolen, Slovenská republika, jdrmla@gmail.com*

ABSTRACT: The article deals with the problem of hydraulic oil contamination, which is the most common cause of hydraulic system failures in industry. We describe an experiment in which, by effectively using a relatively simple measuring device designed for condition monitoring of operating fluids in the hydraulic system which is widely available on the market, we managed to demonstrate and locate the source of contamination and proposed solutions to prevent the problem in the future. By measuring the oil cleanliness, we confirmed the hypothesis that the oil is contaminated due to insufficient filtration of the hydraulic oil in combination with excessive pollution from the external environment in operation area. Additionally, we proved that the gear pumps are more suitable for harsh working conditions then vane pumps. Using the oil cleanliness measurement, we were able to locate the problem and provide the machine operator with feedback based on exact measurement results. In this way, we demonstrated the previous considerations and recommended corrective measures based on the findings.

Key words: condition monitoring, oil cleanliness, laser particle detector, hydraulic oil, hydraulic system, maintenance

ABSTRAKT: Článok sa zaoberá problémom kontaminácie hydraulického oleja, ktorý je najbežnejšou príčinou porúch hydraulických systémov v priemysle. Opisujeme experiment, pri ktorom sme efektívnym využitím pomerne jednoduchého, na trhu dostupného meracieho zariadenia na sledovanie stavu prevádzkových kvapalín v hydraulickom systéme preukázali a lokalizovali zdroj kontaminácie a navrhli tak riešenia ako problému v budúcnosti predchádzať. Meraním čistoty oleja sme potvrdili hypotézu, že olej je kontaminovaný z dôvodu nedostatočnej filtrácie hydraulického oleja v kombinácii s nadmerným znečistením pochádzajúcim z externého prostredia v prevádzke. Okrem toho sme potvrdili, že zubové hydrogenerátory sú vhodnejšie do náročných pracovných podmienok ako lamelové hydrogenerátory. S využitím merania čistoty oleja sme boli schopní problém lokalizovať a poskytnúť prevádzkovateľovi zariadenia spätnú väzbu podloženú exaktnými výsledkami z meraní. Preukázali sme tak predošlé úvahy a odporučili sme nápravné opatrenia vychádzajúce zo zistených poznatkov.

Kľúčové slová: sledovanie stavu, meranie čistoty oleja, laserový detektor častíc, hydraulický olej, hydraulický systém, údržba

INTRODUCTION

While in the past the main tools used to inspect hydraulic systems were inspection and reading data from indicators, today's modern oil analysis applies new, sophisticated tools and devices. A modern system for monitoring the condition of a hydraulic system involves number of strategically important components to be the successfully integrated (Dowson 1998). With the changing construction of industrial equipment, the requirements for their performance are also increasing. Today's hydraulic power units are designed for the highest possible pressure, speed and performance, which naturally increases their operating temperature and demands on the quality of operating fluids (Baczewski and Szczawinski 2016).

Electromagnetically and proportionally controlled directional control valves are used to control the oil flow in the hydraulic circuit of the press machine. These elements are particularly sensitive to the cleanliness of the hydraulic oil in the circuit, as even microscopic impurities can damage or block internal parts, such as sliding spool and control edges, and thus negatively affect the operation of the entire machine. Hydraulic systems, whose moving part tolerances were once 25 to 50 µm, today operate within tolerances of 1 to 5 µm. The elements of the transformation block are therefore particularly sensitive to the cleanliness of the hydraulic oil in the circuit. During their work cycle, they perform either a rotary or a sliding movement, and it is almost always a metal-to-metal action. With clearances of 1 to 5 µm, it is therefore impossible to omit the damage that can be caused by an ordinary grain of sand, which is ten times larger than the clearance (Šupák and Almášiová 2014).

Impurities enter the working fluid in a variety of ways - from the external environment, by the very action of mutually moving surfaces inside each element, while they grow in a geometric series. Although filters ensure their removal, no filter is capable of capturing 100 % of all impurities. Therefore, it is necessary to regularly check the purity of the working fluid, which is especially true in operations with continuous production. The purity of the hydraulic oil is a basic prerequisite for the correct function of any hydraulic mechanism. Oil contamination in the hydraulic system results in wear that reduces the life of all system components, especially functional parts with small clearances. In some elements, due to the influence of dirt, the function may deteriorate or become completely impossible. Sources of impurities can be divided into four basic groups according to their origin:

- **primary impurities** – enter the circuit during filling with liquid and during assembly of individual elements and lines. These are mainly chips from machining, abrasive particles, mixtures from lapping, dust, sand from castings, particles of metals and seals, debris from welds and from heat treatment, paint and other immiscible liquids,
- **impurities from the environment** – they enter the system through the seals of hydraulic elements a through the filling and venting holes of the tank,
- **impurities arising from the function of the system** – products of wear, corrosion, parts of coatings, erosion, or parts of varnishes and paints,
- **impurities arising from the liquid** – they arise from chemical changes in the liquid, oxidation, the effect of temperature and pressure, or they are impurities from the production process and transportation of the hydraulic fluid (Antala 2008).

Impurities in hydraulic oil have the following effect on the function of precise hydraulic elements:

- increase the frictional forces of spools inside the valves, pistons, valve cones due to clogging of clearances and joints with small particles (10 μm),
- cause mechanical erosion of the surfaces of the seats, the edges of the spools, reduce the overlap, change the resistance of the screens, nozzles and clearances in places of high flow velocities,
- particles smaller than the clearance of the components cause wear by abrasion,
- particles larger than the clearance of the components can clog nozzles, screens and completely disable the hydraulic element from functioning,
- particles the size of the joint dimension are the most dangerous because they can cause seizing and sudden failure of the element›s function. (Antala 2008).

In the case of gross contamination, the particle size is greater than 14 μm and the device stops due to seizing. As a result of fine pollution with a particle size of 6 to 14 μm, there is an increase in working clearances and thus a decrease in volumetric efficiency, or to increase in temperature, decrease in viscosity and possible seizure. Very fine pollution with a particle size of 4 to 6 μm, consisting of very small metal particles and refining products, which likewise cause wear of functional surfaces. (Antala 2008).

Precisely for the reason that hydraulic systems are extraordinary sensitive to the condition of the operating fluid, it is necessary to pay adequate attention to their operating condition for their proper function, maximum use of their advantages and maximum compensation of their disadvantages, where tribodiagnostics is offered as an effective preventive maintenance tool. Because like any part of the system, the working fluid – hydraulic oil – requires monitoring of its operating parameters. One of the most important features is its purity. For this reason, it is crucial to carry out regular diagnostics and filtration of oil fillings, which was also confirmed by the research of the authors Tkáč et al. (2021), Hnilicová et al. (2021), where 80% of all hydraulic system failures occur due to hydraulic oil contamination (Stachowiak and Batchelor 2013, Peťková 2012, Kučera and Aleš 2017, Kopčanová et al. 2020).

A common problem in today‘s industrial operations using hydraulic systems is that they do not have sufficient insight into the condition of their operating fluids. Operators are often unaware of the condition monitoring importance and since relatively little attention is paid to this issue, there is still a lack of general awareness of the tools available to address these issues. The aim of the article is to point out that with the help of a relatively simple tool - a particle detector for measuring oil cleanliness, it is possible to effectively locate a fault in the hydraulic system, document the possible causes of the undesirable condition and take adequate corrective measures. (Fitch 2001, Totten et al. 2001)

MATERIAL AND METHODS

In this article, we will focus on locating the problem inside the hydraulic system of the foam press machine, which is included in continuous operation in the automotive industry. The main method will be an experiment, in which we will try to locate the problem in the hydraulic circuit and find out the causes of its occurrence with the help of measuring the cleanliness of the oil. We chose the Parker iCount Oil Sampler (IOS) portable particle monitor to measure impurities in hydraulic oil. The portable particle detector is an innovative solution to the challenge of measuring the quality of hydraulic oils in a wide variety of outdoor and indoor applications, it is a self-contained system, equipped with a laser particle detection counter, battery, oil pump and internal memory with a website generator. Cleanliness can be measured regularly or continuously. The measurement of solid particles takes place using devices working on the principle of a laser. IOS uses light dimming technology. The measured liquid flows between the laser source and the evaluation device. Contaminants in the fluid interrupt the light beam and transmit the image to the photodiode cell, where the resulting change in light intensity leads to a directly proportional change in electrical output. The processor then evaluates the number of particles contained in the sample, and as a result, the liquid is assigned to a purity class according to ISO or NAS standards. Proven laser detection technology guarantees accurate, repeatable, reproducible results and real-time detection of particles down to 4 microns in size. The data is immediately displayed, saved or downloaded to an external device for analysis, further processing or archiving. (Parker, 2015).

The measurement principle is shown in three steps in Figure 1 below:

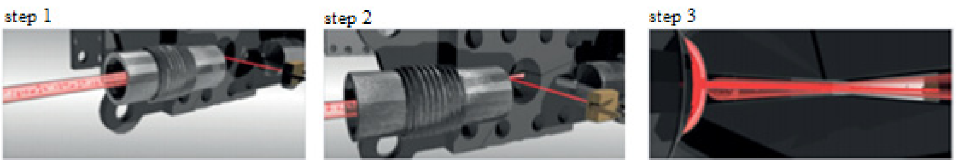

Fig. 1 Description of the process of measuring oil purity with a laser detector
Obr. 1 Popis procesu merania čistoty oleja laserovým detektorom
Source: (Parker 2015)

Step 1: Simply put, a controlled column of contaminated liquid enters the laser optical scanner chamber. The chamber design maintains the distribution of contamination in the liquid.

Step 2: When the liquid reaches the photodiode cell of the IOS meter, a precise laser light is applied and thus projected through the flowing oil column. A laser diode projects an image of the sample onto a photodiode cell.

Step 3: Contaminants in the oil create reflections or shadows that are measurable as a change in the intensity of the light beam. These changes are evaluated by the processor as impurities - their size and number are analysed. (Parker, 2015).

The measured oil purity is then displayed on the device‘s OLED digital display in purity classes according to ISO or NAS, see specification at Table 1. We will evaluate the measurements according to the ISO system, which expresses the number of particles in a given size range. Table 2 below shows the cleanliness limit values for different types of hydraulic elements and Table 3 explains the cleanliness code values according to ISO 4406:2021.

Table 1 Specification of measuring device
Tabuľka 1 Špecifikácia meracieho zariadenia

Feature	Specification
Product start-up time	10 s minimum
Measurement period	Default 30 s run time; 15 s data logging time
Reporting interval	Onboard data storage every second; output via RJ45 connection
Principle of operation	Laser diode optical detection of actual particulates
Working pressure	2.5 – 350 bar
Working viscosity	1 – 300 cSt
Flow range through IOS	40 – 140 $ml.min^{-1}$; controlled 60 $ml.min^{-1}$ by IOS´s internal pump
Ambient storage temperature for unit	-40 °C to +80 °C
Operating temperature for unit	-30 °C to +80 °C
Operating humidity range	5 %RH to 100 %RH
Oil operating temperature	+5 °C to + 80°C
Moisture sensor	Linear scale within the range 5 %RH to 100 %RH

Source: (Parker 2015)

Table 2 Limits values of oil cleanliness for chosen hydraulic elements
Tabuľka 2 Limitné hodnoty čistoty oleja pre vybrané hydraulické prvky

Hydraulic elements	Required purity class according to ISO	Recommended filtration (μm)
Gear pumps	19/17/14	10
Vane pumps	18/16/13	10
Directional control valves	18/16/13	10

Source: (Parker 2015)

Table 3 Code numbers according to ISO 4406:2021
Tabuľka 3 Čísla kódov podľa ISO 4406:2021

Code number	Number of particles in 1 ml	
30	5000000	10000000
29	2500000	5000000
28	1300000	2500000
27	640000	1300000
26	320000	640000
25	160000	320000

24	80000	160000
23	40000	80000
22	20000	40000
21	10000	20000
20	5000	10000
19	2500	5000
18	1300	2500
17	640	1300
16	320	640
15	160	320
14	80	160
13	40	80
12	20	40
11	10	20
10	5	10
9	2,5	5
8	1,3	2,5
7	0,64	1,3
6	0,32	0,64
5	0,16	0,32

Source: (ISO 4406: 2021)

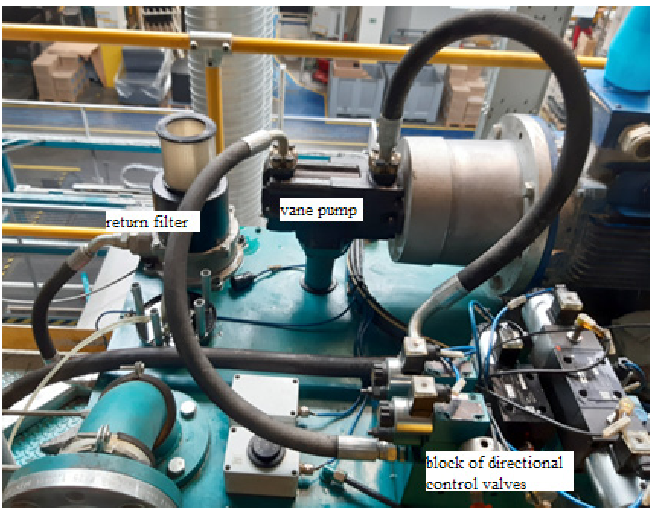

Fig. 3 Vane pump and return filter on Press Machine EPDM
Obr. 3 Lamelový hydrogenerátor a spätný filter na lise EPDM
Source: author

Fig. 4 Gear pump and control block on Press Machine HA-40
Obr.4 Zubový hydrogenerátor a riadiaci blok na lise HA-40
Source: author

RESULTS

In this experiment, with the help of oil purity measurement, we aimed to reveal the failure behaviour of hydraulic press machines on a production line producing carpets with a foam layer used to cover the floor of passenger cars. The workplace consists of seven press machines that gradually produce foam interior parts. Hydraulic circuits are the source of power for each of these machines, which press the required products using hydraulic cylinders. The hydraulic presses showed irregular failure behaviour during their operation – the machine showed an error mode, the hydraulic cylinders did not extend smoothly, or did not reach the set position, the machine got stuck during operation, etc. The malfunctions appeared repeatedly and irregularly.

For this reason, we first checked the operating conditions of the machines and then proceeded to measure the purity of the oil. Oil purity was measured with a Parker iCount Oil Sampler measuring device at a total of 7 workplaces. Hydraulic oils of an unspecified brand, type ISO VG 46, were used in the hydraulic power units of the machines.

A vane pump was installed in the hydraulic circuit of the Press Machine EPDM, see Figure 3, for the operation of which the oil cleanliness limits are 18/16/13 with a recommended filtration of 10 μm. The code number 18/16/13 means that 1300-2500 particles larger than 4 μm, 320-640 particles larger than 6 μm and 40-80 particles larger than 14 μm are found in 1 ml of liquid. In the Press Machines HA-40, see Figure 4, gear pumps were installed, for the operation of which the limit values of oil cleanliness are 19/17/14 with a recommended filtration of 10 μm. The code number 19/17/14 means that 2500-5000 particles larger than 4 μm, 640-1300 particles larger than 6 μm and 80-160 particles larger than 14 μm are found in 1 ml of liquid. To control the flow of hydraulic fluid, electromagnetically controlled directional control valves were used in both types of presses, which require an oil cleanliness of up to 18/16/13 with a recommended filtration of 10 μm, which means that 1 ml of fluid can contain 1,300-2,500 particles larger than 4 μm, 320-640 particles larger than 6 μm and 40-80 particles larger than 14 μm. In the evaluation of the measurement in Table 4, the measured values of oil cleanliness are recorded. The values are given according to the ISO 4406:2021 system, which expresses the number of particles in a given size range. MARINESCU et al. (2021) analysed the contamination level of the hydraulic oil used on an endurance stand for testing two different types of gear pumps. The results of the analysis are consistent with our results. Also researches KRILEK et al. (2019) and OSMANOVIC et al. (2018) evaluated hydraulic oil samples in his article and reports cleanliness level, which are close to our measured values.

Table 4 Results from oil purity measurement
Tabuľka 4 Výsledky merania čistoty oleja

	Machine	4µm	6µm	14µm	Note – hydraulic elements used
1	Press Machine EPDM	*	21	14	vane pump
		*	21	14	directional control valves
2	Press Machine HA-40 (1)	19	17	13	gear pump
		19	17	13	directional control valves
3	Press Machine HA-40 (2)	21	19	16	gear pump
		21	19	16	directional control valves
4	Press Machine HA-40 (3)	19	16	13	gear pump
		19	16	13	directional control valves
5	Press Machine HA-40 (4)	19	16	13	gear pump
		19	16	13	directional control valves
6	Press Machine HA-40 (5)	21	19	15	gear pump
		21	19	15	directional control valves
7	Press Machine HA-40 (6)	21	19	18	gear pump
		21	19	18	directional control valves

* measured purity of the oil in the given category exceeds the measurement limit values

Values highlighted in red exceed the required cleanliness class

Values highlighted in green meet the required cleanliness class for the given element

Source: author

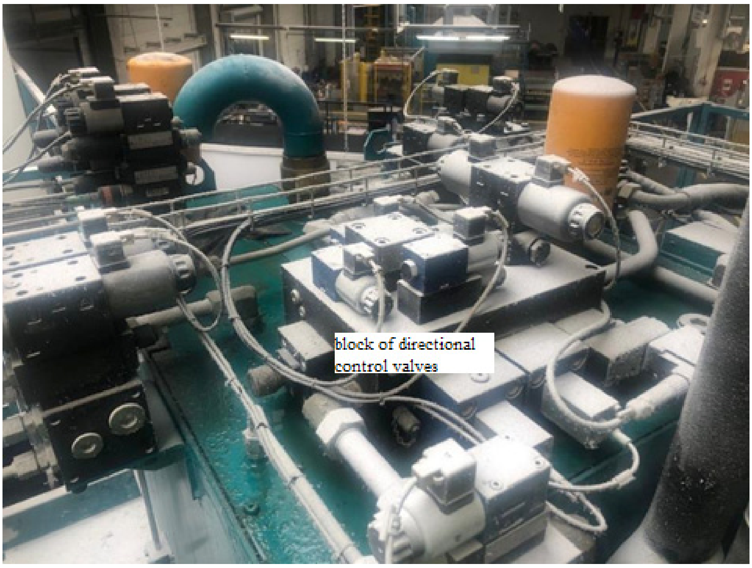

Fig. 5 Contaminated control block on Press Machine EPDM
Obr. 5 Znečistený riadiaci blok na lise EPDM
Source: author

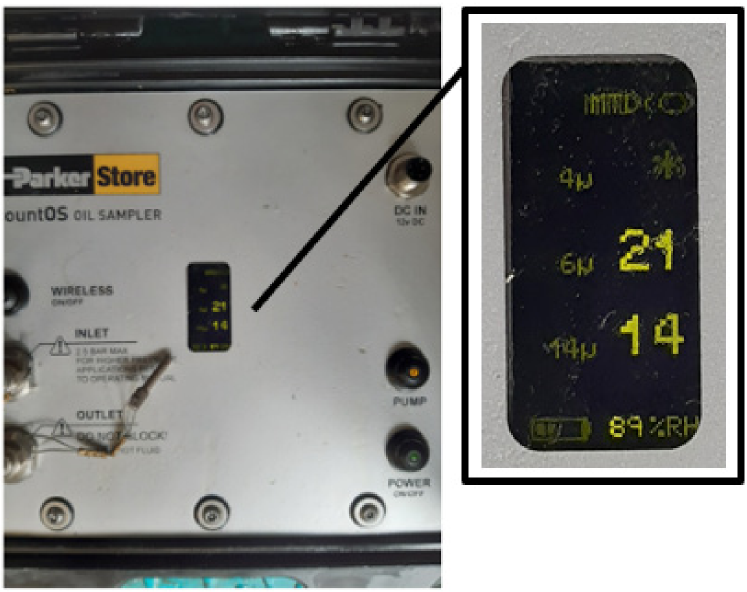

Fig. 6 Measured oil clenliness values on the Parker IOS instrument
Obr.6 Namerané hodnoty čistoty oleja na meracom zariadení Parker IOS
Source: author

CONCLUSION

Through observation, it was found that the individual hydraulic circuits were not equipped with filters of the prescribed filtration efficiency and, moreover, the operation itself was a source of excessive pollution. In the production of textile parts of products, a fine, white, dusty substance is used, which is present in the air. Directional control valves, see Figure 5 and pistons of the hydraulic cylinders were covered with this substance. During the movement of these elements, contaminants from the air penetrate through the seals into the interior of the hydraulic elements. Experimental measurements have shown that the hydraulic circuits of the press machines were contaminated by this pollution, as seen in the Table 3 and Figure 6. Values exceeding the specified limits for the given category are marked in red colour. It is clear from the measurement results that the exceeded limits are mainly for particles with a smaller size. Such contamination of hydraulic oil is unsuitable for the reliable operation of hydraulic systems. While gear pumps are able to work even with slightly contaminated hydraulic oil, vane pumps or directional control valves no longer do.

This is precisely why we have observed irregular operation, blocking of hydraulic cylinders and resulting malfunctions on Press Machines HA-40 (1, 2, 5 and 6). The gear pumps on these presses were able to work without a problem even with this level of oil contamination. However, it should be noted that they are exposed to excessive wear and failure of these elements can also be expected in the future. With the Press Machines EPDM, the problem was already manifested with the vane pump, which, due to its design, is more sensitive to the purity of the oil. In addition, the cleanliness values were the worst at this workplace, unmeasurable with a particle size of 4 μm – that means, outside the measuring range. The vane pump was overheating and making excessive noise. It was also refurbished in the past. The control elements of this press were also in the worst condition, by experiment we discovered a distributor with a blocked sliding spool.

Based on the experiment results we can conclude that the gear pumps used in Press Machines HA-40 (1, 2, 5 and 6) work more reliable under difficult working conditions with slight contamination of hydraulic oil, however, the vane pump used in Press Machines EPDM is considered to be a less reliable choice for working in harsh environments. In ideal working conditions, none of the pumps should be exposed to contaminated oil but in real working process, one can hardly ensure that. Sor this reason, use of gear pumps in dirty working environments is more appropriate. Considering the directional control valves, to ensure their optimal working performance, the cleanliness needs to be ensured in any case. In this particular application, a protecting cover or other technical counter measures would be in place. Additionally, by consistently filtering the oil using a filter cart, replacing the filter inserts with ones of better quality and ability to capture smaller particles, and paying attention to the cleanliness of the hydraulic components, it is possible to eliminate the revealed problems. In addition to the cleanliness of the oil, it is also necessary to pay attention to the cleanliness of the equipment itself, through which the contamination enters the oil circuit. Based on this output from the measurement, it is possible to plan the necessary corrective measures and repeat the measurement after a few months until the effect becomes apparent. Subsequently, it is advisable to introduce periodic monitoring of the condition of operating fluids.

ACKNOWLEDGMENT

This research was supported by the Slovak Research and Development Agency under the Contract no. APVV-21-0180.

LITERATURE

ANTALA, J. 2008. Hodnotenie znečistenia oleja. Strojárstvo, vol.1, no 9, pp. 194-195.

DOWSON, D. *1998. History of Tribology. Hoboken: Wiley.*

FITCH, J. C. 2001. Advancements in Fluid Analysis Technologies and Strategies for Hydraulic System Condition-Based Maintenance. In: Hydraulic Failure Analysis: Fluids, Components, and System Effects. West Conshohocken: ASTM.

ISO 4406: 2021. ISO 4406:2021 Hydraulic fluid power — Fluids — Method for coding the level of contamination by solid particles.

PARKER, 2015. icountOS: Accurate Condition Monitoring made Quick, Simple and Cost Effective.

PEŤKOVÁ, V. et al. 2012. Tribotechnika v teórii a praxi. Košice: Vienala, 2012. s. 366 s. ISBN 978-80-8126-0575.

STACHOWIAK, G., BATCHELOR, A. W. 2013. Engineering Tribology. 4. vydanie. Oxford: Butterworth-Heinemann.

ŠUPÁK, M., ALMÁŠIOVÁ, J. 2014. Hydraulické mechanizmy. first ed. Bratislava: Metodicko-pedagogické centrum v Bratislave.

TOTTEN, G. E., WILLS, D. K., FELDMANN, D. G. 2001. Hydraulic Failure Analysis: Fluids, Components, and System Effects. West Conshohocken: ASTM.

BACZEWSKI, K., SZCZAWINSKI, P. 2016. Investigation of the process of ageing of hydraulic oil during its use. In The Archives of Automotive Engineering – Archiwum Motoryzacji, vol 73, no. 3, pp. 5 – 18. *DOI:10.14669/ AM.VOL73.ART1*

HNILICOVÁ, M., TURIS, J., HNILICA, R. 2021. Application of Multidimensional Statistical Analysis in Tribotechnical Diagnostics of Hydraulic Fluids in Woodworking Equipment. In Materials, vol. 14, 22 pp.

TKÁČ, Z., ČORNÁK, Š., KOSIBA, J., JANOUŠKOVÁ, R., MICHALIDES, M., VOZÁROVÁ, V., CSILLAG, J. 2021. Investigation of degradation of ecological hydraulic fluid. In Proceedings of the Institution of Mechanical Engineers: Part C – Journal of Mechanical Engineering Science (In press).

KOPČANOVÁ, S., SEJKOROVÁ, M., KUČERA, M., HNILICOVÁ, M. 2020. Wear of hydraulic system components assessment based on the analysis of hydraulic oil degradation degree. In Przemysel Chemyszny, vol. 99, no.9, pp. 1000 – 1004.

KUČERA, M., ALEŠ. Z. 2017. *Morphology Analysis of Friction Particles* Generated *in Tractor Transmission Oils*. In Acta Technologica Agriculturae, vol. 20, no.3, pp. 57–62.

KRILEK, J., KOVÁČ, J., KUVIK, T., DOBROTOVÁ, L. 2019. Analysis of hydraulic oil to drive band sawmill. In Scientific Bulletin of UNFU, vol. 29, no 10, pp.89 – 92. ISSN 1994-7836.

MARINESCU, A.D., RADULESCU, A.V., RADULESCU, I. 2021. Researches concerning the hydraulic oil degradation process in gear pumps. In Journal of Research and Innovation for Sustainable Society (JRISS), vol. 3, no. 2, pp.43-52. DOI: 10.33727/JRISS.2021.2.5:43-52

OSMANOVIC, A., TRAKIC, E., SARIC, B., HADZISMAJLOVIC, M., BECIROVIC, M. 2018. Diagnostics of hydrostatic power transmission on hydraulic excavators, using work fluid analysis. In Technics – Technologies – Education – Management : Journal of Society for Development of Teaching and Business Processes in New Net Environment in B&H, vol. 13, no. 3, pp. 115 – 120. ISSN 1840 – 1503.

Corresponding author:
Jakub Drmla, phone +421 948 777 493, e-mail: jdrmla@gmail.com

ACTA FACULTATIS TECHNICAE XXVII
ZVOLEN – SLOVAKIA 2022

METHOD OF MEASURING AND EVALUATING VIBRATION DURING MILLING OF WOOD-BASED MATERIAL ON A CNC MACHINE IN MATLAB

METÓDA MERANIA A VYHODNOCOVANIA VIBRÁCIÍ PRI FRÉZOVANÍ MATERIÁLU NA BÁZE DREVA NA CNC STROJI V MATLABE

Áron Hortobágyi, Peter Koleda

Department of manufacturing and automation technology, Faculty of technology, Technical university in Zvolen, T. G. Masaryka 24, 960 01, Zvolen, Slovak republic, xhortobagyi@is.tuzvo.sk, peter.koleda@tuzvo.sk

ABSTRACT: Subject of research was to find strategy for effective evaluation of vibrations measured on grippers of CNC during MDF board milling. Multiple strategies were tried out, such as single axis signal assessment, combination of three axes on one timeline, and separate evaluation of axis pairs measured on two grippers simultaneously. Although having multiple axes plotted together seemed to be sufficient for amplitudes from accelerometer, same result performed poorly after fourier transform – dominant frequencies overlapped, and maxima were hard to read. Problem was bypassed by plotting table with dominant frequency maximas. Scripts were also developed for assessment of multiple measurements with output saved in .xlsx format and to assess signal in smaller sections. These allow to quickly summarize all data, and to provide closer views on sections of signal, where amplitudes maxima reach relatively similar values.

Key words: Matlab, Fourier transform, Picoscope

ABSTRAKT: Predmetom výskumu bolo nájsť stratégiu pre efektívne vyhodnotenie vibrácií nameraných na prísavkách na CNC pri frézovaní MDF dosky. Vyskúšalo sa viacero stratégií, ako vyhodnocovanie signálu z jednej osi, kombinácia troch osí na jednej časovej osi a samostatné vyhodnotenie párov osí meraných na dvoch prísavkách súčasne. Viac osí vynesených spolu sa ukazovalo ako postačujúce vyhodnotenie pre amplitúdy z akcelerometra, ale rovnaký výsledok po Fourierovej transformácii sa ukázal ako nevhodný – dominantné frekvencie sa prekrývali a maximá boli ťažko čitateľné. Problém bol vyriešený vynesením tabuľky s uvedenými maximami dominantných frekvencií. Ďalej boli vyvinuté aj skripty na vyhodnotenie viacerých meraní s výstupom vo formáte .xlsx a na vyhodnotenie signálu v menších úsekoch. Tieto umožňujú rýchlo zhrnúť všetky údaje a poskytnúť bližší pohľad na úseky signálu, kde maximá amplitúd dosahujú relatívne podobné hodnoty.

Kľúčové slová: Matlab, Fourierova transformácia, Pikoskop

INTRODUCTION

The article is about vibration evaluation strategies in Matlab. In the research, fast Fourier transform was used. Its computation for spectral analysis was described by (Ninness, 2010). Picoscope, used in this research was already used for experiments, such as verification of linear dynamics of falling impact on flooring material (Philip, Löfgren, 2018).

The measurement of vibration during machining process is already well explored topic. It could be performed with use of machine vision (Sandak, Orlowski, 2018). Research on router feed speed control with measurement of acoustic emission was done by (Cyra et al., 1996). Similar work continued, with aim at adaptive control system for CNC router (Iskra, Hernández, 2010). Measurement of tool vibration with use of piezoelectric transducer was addressed by (Karpavičius, Paulius, 2021)

Important difference is the place, where vibrations were measured. The point of interest in this article is pneumatic gripper, holding an MDF board. Mode vibrations of MDF board with use of the harmonic method to static identification of resonant frequencies were studied by (Kaczmarek et al., 2014).

MATERIAL AND METHODS

The article is focused on evaluation techniques of acquired data. Data was gathered during milling process at CNC, with acceleromer probe magnetically attached to vacuum gripper. NVH Diagnostics kit with TA 143 acceleromer and Picoscope PS 4425 4 channel scope was used for measurement. Grippers, NVH kit and acceleromer attachment are shown in fig. 1.

a) b) c)

fig. 1. Measurement assembly. a) pneumatic grippers (G1-G4), b) magnetic attachment of acceleromer, c) NVH kit with PicoScope

obr. 1. Meracia zostava. a) upínacie prísavky (G1-G4), b) magnetické upnutie akcelerometra, c) súprava NVH so zapojením do pikoskopu

Results were displayed in PicoScope 6 software, and saved in .TXT format. Example of received signal is shown in fig. 2.

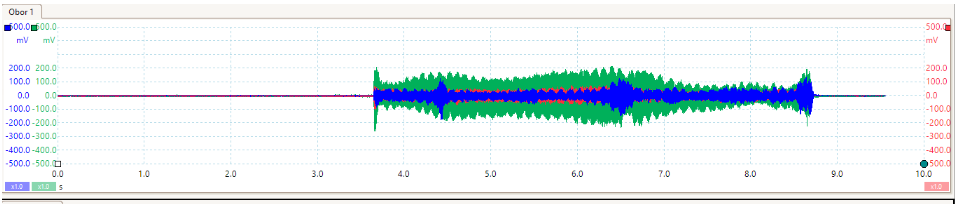

fig. 2. Example of PicoScope software output
obr. 2. Príklad výstupu merania v softvéri PicoScope

As shown in fig. 2, signal consisted of desired data, but I also contained unwanted measurements of vibrations before and after milling process (0 – 3.5 s, 8.7 – 9.5 s). Each color represents an axis. In case of fig. 2, axes are: blue – x, red – y, green – z.

First step in Matlab was to recreate signals. To do so, data had to be loaded from table and plotted. In the first variant, script was created to assess one axis at a time.

```
c=tab.c;
x=tab.x;
plot (c,x);
```

To find dominant frequencies, Fourier transform was carried out. These were plotted next to output signal. The source script was (MATHWORKS, 2012):

```
L=length(X);
Fs = sampling_frequeny;
T = 1/Fs;
t=(0:L-1)*T;
Y=fft(X);
P2 = abs(Y/L);
P1 = P2(1:L/2+1);
P1(2:end-1) = 2*P1(2:end-1);
f = Fs*(0:(L/2))/L;
plot(f,P1);
title(„Single-Sided Amplitude Spectrum of S(t)“);
xlabel(„f (Hz)“);
ylabel(„|P1(f)|“);
```

Result of this script can be seen in fig. 3.

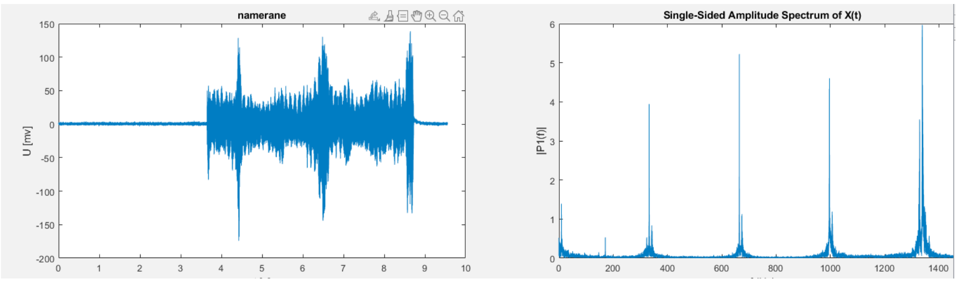

fig. 3. Amplitudes and fourier transform of one axis signal
obr. 3. Amplitúdy a fourierova transformácia signálu z jednej osi

Next step was to assess all three axes in one chart. To do so, hold function was used, as well as color coding of axes.

```
plot (c,z,'Color',[0,1,0,0.2]);
hold on;
plot (c,x,'Color',[0,0,1,0.2]);
plot (c,y,'Color',[1,0,0,0.15]);
hold off;
```

Another part of script was added, to cut off irrelevant signal segments. Irrelevant part was described as signal, where no value exceeds -7 mV. Therefore, relevant part was between first and last value exceeding the set limit. After signal was cut, time values also had to be rearranged, so the data would begin at time 0 seconds.

```
c=tab.c;
%find begining
begining=find(tab{:,2}<-7,1);
%find end
end=find(tab{:,2}<-7);
end=end(length(end),1);
%cut end
tab(end:length(tab.c),:) = [];
%cut begining
tab(1:begining,:) = [];
%change time values
c(length(tab.c)+1:length(c))=[];
tab.c=c;
```

Result of this script can be seen in fig. 4.

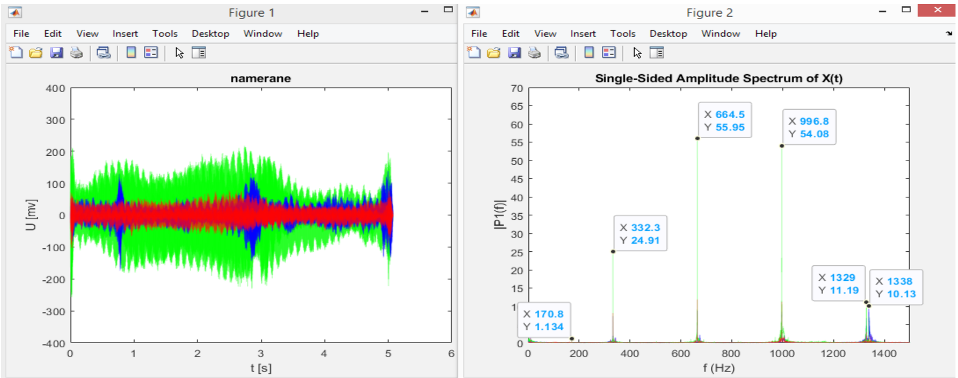

fig. 4. Shortened signal of three axis and Furier transforms with hand-marked maxima
obr. 4. Skrátený signál z troch osí, Fourierova transformácia s ručne označenými maximami

In this layout, amplitudes are much easier to compare. Another useful feature of chart is box with values shown when clicked. This is very useful to fing exact maxima. However, when working with multiple charts, this proved to be time consuming method. Also, overlaying peaks were hard to pinpoint. Another part of script was added, so these values would be shown in table next to charts.

```
%find all results larger than 5
max_P1=find(P1>5);
frekv=zeros(length(max_P1),1);
maxima=zeros(length(max_P1),1);
frekv=f(max_P1);
maxima=P1(max_P1);
frekv=frekv';
vystup2=table(frekv,maxima);
dec=floor((round(frekv,2)-floor(frekv))*100)
frekv=floor(frekv);
vystup=table(frekv,dec,maxima);
%show table---
uitable(,Data',vystup{:,:},'ColumnName',{,f' ,,' ,ZA'},'-
ColumnWidth',{30,20,45},'Units', ,Normalized', ,Positi-
on',[0.74 0.5 0.115 0.5]);
```

The script finds all values larger than 5. In most cases, there are several results arround the dominant frequency. To make tables easier to read, only highest number from the group is shown as a result. Output of this change can be seen in fig. 5.

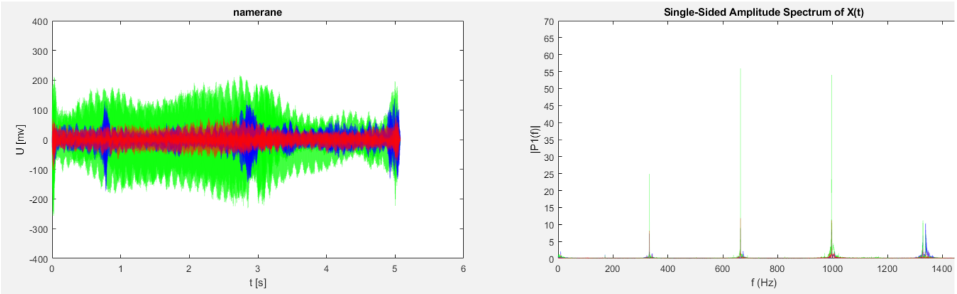

	f	,	X
1	332	35	7.3009
2	664	70	8.7429
3	996	85	8.4859
4	1339	4	10.3863

	f	,	Y
1	332	35	8.1645
2	664	50	11.8539
3	996	85	11.2170

	f	,	Z
1	332	35	24.9063
2	664	50	55.9521
3	996	85	54.0767
4	1329	20	11.1904

fig. 5. Addition of tables with calculated maxima
obr. 5. Doplnenie tabuliek s vypočítanými maximami

Next step brought a change in measurement methodology. As PicoScope allowed measurement of our axes simulateously and y axis showed smallest output in all previous measurements, it could be excluded. Instead, two grippers were measured simulateously, two axes on each. PicoScope output is shown in fig. 6.

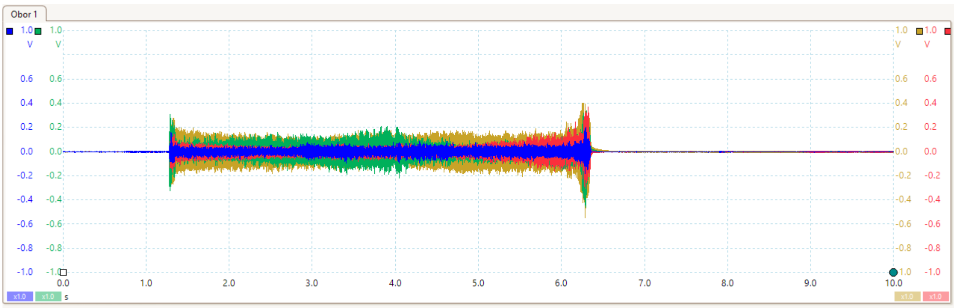

fig. 6 Simulateous measurement of two grippers
obr. 6. Súčasné meranie na dvoch prísavkách

There were four signals in a chart which made it difficult to interpret each axis. Therefore, another script was designed to divide signals and transforms into two charts, each corresponding to one gripper. Some of recieved results were in V insead of mV, so script had to detect units, and if needed, convert everything into mV:

```
if and(tab{1,2}~=0,and(abs(tab{1,2})<0.01,ab-
s(tab{2,2})<0.01))
    tab.xa=tab.xa*1000;
end
```

RESULTS

Result of splitting signal in accordance to gripper is shown in fig. 7.

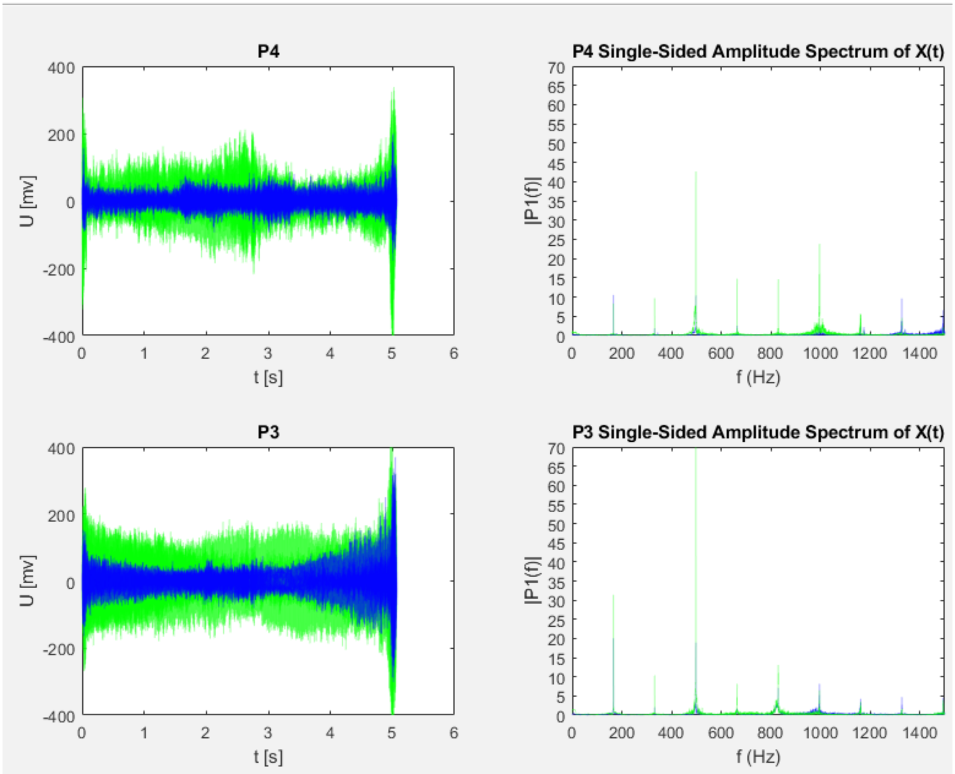

f	,	XA
165	94	20.0547
498	25	18.9261
829	76	7.1221
996	12	8.1575

f	,	ZA
166	15	8.3098
332	11	9.7174
498	25	42.6188
664	21	14.7498
830	16	14.6501
996	32	23.8225
1161	28	5.7229

	f	,	XA
1	165	94	10.5482
2	498	25	10.3864
3	1327	83	9.6424
4	1494	19	6.5960

f	,	ZA
166	15	31.3988
332	11	10.3617
498	6	77.5103
664	21	8.1417
829	76	13.1215
996	12	6.4628

fig. 7. Assessed signal from simulateous measurement on two grippers. X axix - blue, Z axis – green, P4 – gripper 4, P3 – gripper 3
obr. 7. Vyhodnotenie signálu zo súčasného merania na dvoch prísavkách. Os x – modrá, os z – zelená, P4 – prísavka 4, P3 – prísavka 3

The results were already in form easy to interpret. The last step was to enable assessment of multiple measurements in one run. Another script was developed to create a list of files in folder and assess all of them. To make mathematical evaluation easier, maximas of dominant frequencies were exported into excel chart (Table 1) :

```
if exist(‚excel','var')==1
   writematrix(nazvy(poradienazvu).name,'excel.xlsx','Shee
   t',1,'Range',excel(excelriadok,excelstlpec));
   writetable(vystup2,'excel.xlsx','Sheet',1,'Range',
   excel(excelriadok,excelstlpec+1));
   excelstlpec=excelstlpec+2;
end
```

Table 1. FFT output in excel
Tabuľka 1. výstup FFT v programe excel

m10.txt	**X (G4)**	**X (G4)**	**Z (G4)**	**Z (G4)**	**X (G3)**	**X (G3)**	**Z (G3)**	**Z (G3)**
	frekv	**maxima**	**frekv**	**maxima**	**frekv**	**maxima**	**frekv**	**maxima**
	332.28	9.81	1.58	5.67	332.28	23.08	1.10	6.77
	664.56	83.28	332.28	46.03	664.72	148.69	332.28	34.21
	997.01	25.95	664.56	182.20	996.85	26.51	639.03	5.04
	1329.13	19.97	997.01	20.43	1329.29	9.68	664.72	255.37
			1329.13	6.47			690.26	5.00
							1005.99	17.80
							1329.29	7.58

Another type of assessment would be examination smaller signal segments. To enable such evaluation, script was written to split signal in second intervals, plot the signal, fourier transform results, and dominant frequency maxima:

```
%set amount of sections
seconds=length(tab.c)/sampling_frequency;
section=seconds/round(seconds);
tab2=tab; %save table
figure(1);
tiledlayout(round(seconds),3);
tile=0;

for i=0:usek:(seconds-section)
    tab=tab2;%load table
    fig=fig+1;
    tab(round((i+section)*sampling_frequency):length
    (tab.c),:) = [];%cut end
    if i~=0
        tab(1:round(i*sampling_frequency),:) = [];
    end
```

Result of the script is shown in fig. 8. The original signal before splitting is shown in fig. 4 and fig. 5.

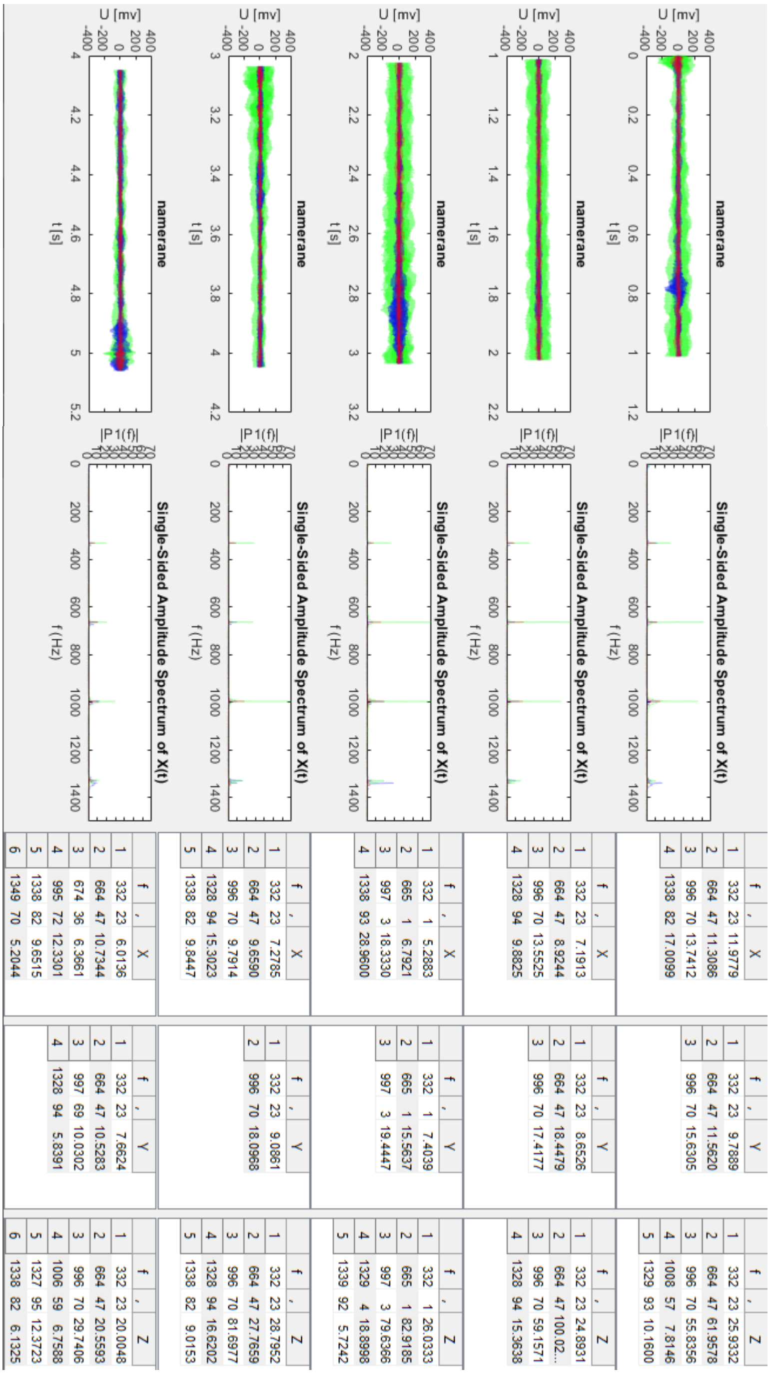

fig. 8. Signal cut into second intervals
obr. 8. Signál rozdelený do sekundových intervalov

DISCUSSION

As seen in results, an assessment tool was developed for signals received via PicoScope. Matlab was chosen as platform for the tool, as the program was suitable for mathematical tasks and could be expanded with use of scripts, and these could be later used in simulations in Simulink (Karban, 2006). Another reason was an in-built fourier transform function already available (Ninness, 2010).

First scripts resulted in chart of dominant frequencies and amplitude changes at one axis (fig. 3). It was readable, but such evaluation would require large number of co-dependent charts. Therefore, three axes were combined (fig.4, fig. 5) and peaks of each dominant frequencies were programmed to be shown in result charts. However, if data comparison between multiple measurements was needed, this method would not be effective. Therefore, script for evaluation of multiple measurements was designed (tab. 1). Also, previous scripts were changed to evaluate data from simultaneous measurement on two grippers (fig.7). Lastly, script for evaluation of signal sections was written (fig. 8).

The achieved results provide a solid basis for data evaluation, there are multiple point that could enhance the program.

First, measured amplitudes were so far coded to be shown in mV. This can be easily changed by relation (Pico Technology, 2013):

$$100\,mV = 9.81 m \cdot s^{-2} \tag{1}$$

Future research will be pointed to exploration of possibilities of adaptive control of CNC. If the control should be online, there is need for direct link between PicoScope accelerometer and Matlab, without use of .txt save files.

This task will be possible due to compatibility between these platforms, as well as code examples published by (Mathworks, 2014). These were already tested, with result shown on fig. 9. In the test code, acceleration of x axis was measured for 3,5 s.

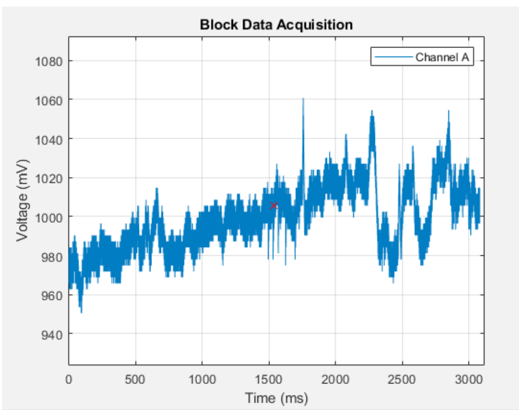

fig. 9. Result of compatibility test between Matlab and PicoScope
obr. 9. Výsledok testu komability Matlabu a Picoscopu

CONCLUSION

Main goal of the research was to create tool for assessment of measured vibrations. For this purpose, Matlab was chosen as a base program. Scripts were prepared for multiple tasks, such as evaluation of three measured axes, evaluation of simultaneous measurement on two grippers and evaluation of multiple measurements with output listing dominant frequencies and their maxima in .xlsx format. Separate script was prepared for evaluation of signal in smaller time sections.

This already provides sufficient tool for evaluation of measured vibrations. Future study will be focused on interconnecting Matlab and PicoScope platforms directly. Another point in future research will be measurement of surface roughness of cut samples and search for connection between the parameters, as it was done by (Iskra, Hernández, 2010).

ACKNOWLEDGMENT

The research was conducted through project APVV-20-0403: FMA analýza potenciálnych signálov vhodných pre adaptívne riadenie nestingových stratégií frézovania aglomerátov na báze dreva

REFERENCES

SANDAK, J., ORLOWSKI, K. A. 2018. Machine vision detection of the circular saw vibrations. *Journal of Machine Engineering*., 18, (3), s. 67–77. Available on: https://bibliotekanauki.pl/articles/100155

KACZMAREK, A., JAVOREK, L., ORLOWSKI, K. 2014. Mode vibrations of plates - experimental analysis. *Annals of Warsaw University of Life Sciences - SGGW. Forestry and Wood Technology*, vol. 88, s. 97 – 101. Available on: https://scholar.google.com/citations?view_op=view_citation&hl=sk&user=J6juwdsAAAAJ&cstart=20&pagesize=80&citation_for_view=J6juwdsAAAAJ:ZHo1McVdvXMC

NINNESS, B. 2010. Spectral Analysis using the FFT. *Department of Electrical and Computer Engineering, The University of Newcastle, Australia*. Available on: http://entsphere.com/pub/pdf/Papers/Signal%20Processing/Spectral%20Analysis%20using%20FFT%20in%20Matlab.pdf

PHILIP, R., LÖFGREN, H. 2018. Experimental Verification of an Instrument to Test Flooring Materials. In *IOP Conference Series: Materials Science and Engineering* (Vol. 310, No. 1, p. 012121). IOP Publishing. Available on: https://iopscience.iop.org/article/10.1088/1757-899X/310/1/012121/meta

KARPAVIČIUS, P. 2021. *Research and development of a universal wireless sensor for cutting tool condition monitoring* (Doctoral dissertation, Kauno technologijos universitetas). Available on: https://epubl.ktu.edu/object/elaba:104016414/

ISKRA, P., HERNÁNDEZ, R. E. 2010. Toward a process monitoring and control of a CNC wood router: Development of an adaptive control system for routing white birch. *Wood and Fiber Science*, 523-535. Available on: https://wfs.swst.org/index.php/wfs/article/view/567

CYRA, G., TANAKA, C., NAKAO, T. 1996. On-line control of router feed speed using acoustic emission. *Forest Products Journal*, *46*(11/12), 27. Available on: https://www.proquest.com/docview/214628450?pq-origsite=gscholar&fromopenview=true

KARBAN, P. 2006. *Výpočty a simulace v programech Matlab a Simulink*. Computer Press, a.s., Brno, 2006. 220 p. ISBN 80-251-1301-9

MATHWORKS, 2014. PicoScope Support from Instrument Control Toolbox. [online] [cit. 2022-10-05]. Available on: https://www.mathworks.com/hardware-support/picoscope.html

MATHWORKS, 2012. Fast Fourier transform. [online] [cit. 2022-09-25]. Available on: https://www.mathworks.com/help/Matlab/ref/fft.html

Pico Technology Ltd. 2013. Three Axis Accelerometer Kit - Quick Start Guide. [online] [cit. 2022-10-05]. Available on: https://www.picotech.com/download/manuals/ThreeAxisAccelerometerKitQSG.pdf

Corresponding author:
Ing. Áron Hortobágyi, tel.: +421 455 206 566, e-mail: xhortobagyi@tuzvo.sk

ACTA FACULTATIS TECHNICAE XXVII
ZVOLEN – SLOVAKIA 2022

FRICTION AND PRESSURE EFFECT ON DISC BRAKE STABILITY USING THE COMPLEX EIGENVALUE METHOD

EFEKT TRENIA A TLAKU NA STABILITU KOTÚČOVEJ BRZDY POMOCOU KOMPLEXNEJ ANALÝZY VLASTNÝCH ČÍSIEL

Ing. Lukáš Hudec[1]

[1]Department of Mechanics, Mechanical Engineering and Design, Faculty of Technology, Technical University in Zvolen, Studentska 26, 960 01, Zvolen, Slovak Republic, xhudecl@is.tuzvo.sk

ABSTRACT: In this paper, an approach to evaluate disc brake stability using the Complex eigenvalue analysis (CEA) is shown. The CEA is the leading method used for revealing complex modes of the braking system and helps to predict brake squeal occurrence. The complex modes occur when the system matrices become asymmetric and the resulting mode deformation consist of a real damping part and imaginary phase part. These unstable modes have a strong inclination to generate brake squeal as observed by numerous researchers. In this paper, design parameters such as the contact friction between pads and disc are evaluated along with their contribution to brake instability. The brake assembly shown in this paper is a vented disc brake typical in many commercial cars today, with and equally common brake pad design. On top of that, the piston pressure is also shown to contribute significantly to system instability. The change in friction coefficient has shown to give rise to more unstable frequencies and change the frequency spectrum substantially.

Keywords: CEA, brake, FEM,

ABSTRAKT: V tomto článku je znázornený prístup k hodnoteniu stability brzdy s plávajúcim strmeňom pomocou komplexnej analýzy vlastných hodnôt (CEA). CEA je popredná metóda používaná na odhalenie komplexných režimov brzdového systému a pomáha predpovedať výskyt pískania bŕzd. Komplexné režimy nastávajú, keď sa matice systému stanú asymetrickými a výsledná deformácia režimu pozostáva z reálnej tlmiacej časti a imaginárnej fázovej časti. Tieto nestabilné režimy majú silnú tendenciu generovať pískanie bŕzd, ako to pozorovali mnohí výskumníci. V tomto článku sú hodnotené konštrukčné parametre, ako kontaktné trenie medzi doštičkami a kotúčom spolu s ich príspevkom k nestabilite bŕzd. Zostava brzdy tu zobrazená má vetraný dizajn s rebrami. Jedná sa o typické prevedenie, ktoré sa nachádza u mnohých dnešných komerčných automobiloch s rovnako bežným dizajnom brzdových doštičiek. Okrem toho sa ukázalo, že tlak piestu tiež významne prispieva k nestabilite systému. Ukázalo sa, že zmena koeficientu trenia vedie k nestabilnejším frekvenciám a podstatne mení frekvenčné spektrum.

Kľúčové slová: CEA, brzda, MKP

INTRODUCTION

Disc brake squeal is an ever-present problem in the automotive industry, at best it is an unwanted irritant and at worst a potential indicator of a larger problem with the brake pads. Brake squeal is defined as noise generated in higher frequency ranges, typically greater than 1 kHz, while other noises, such as whine, occur at lower frequencies and are usually caused by a "stick-slip" (Mills, H. R 1938) phenomenon, during which the additional energy is generated by the system, the cause of which is the frictional force as a function of speed. High-frequency noise is produced when the vehicle is braking, and assuming that the brake pad is not in bad condition, the screeching can be attributed to the coupling mechanism of the complex modes of the disc shapes. A large amount of literature on this topic indicates that the phenomenon of "mode-coupling" is the primary cause of the onset of brake squeal (Nouby et al. 011)(Park, J. S. et al. 2012)(Lv, H. M. et al. 2013)(De Simone, M. et al. 2018), and therefore it is of primary importance to separate the complex modes, so to speak, by targeted structural modification of brake parts. This process is part of the automotive industry's NVH (noise, vibration, harshness) testing process for proposed brakes.

A large amount of research has already been done on the "mode-coupling" phenomenon. Research to eliminate brake squeal began around 1930 (Mills, H. R 1938)(Lamarque, P. et al. 1938) with a focus on experimental methods on brakes, followed by the design of simple discrete numerical models. Later, as a result of the increase in available computer computing power, discretization into finite elements using the finite element method was significantly improved. CEA and dynamic transient analysis, which work on the basis of FEM, are today the basic methods of predicting brake squeal in the automotive industry. CEA is preferred for the lower computational requirements and its connection to the modal space. Where, unlike the FEM formulation, the solution consists of a set of independent equations. Among the first published papers on complex eigenvalue analysis and its application to a braking system were (Liles et al. 1989).

The CEA result provides us with information about the instability on the frequency spectrum and the complex shapes of the disk modes. To predict brake instability, in this work, CEA analysis is performed on an assembly consisting of a brake disc, brake pads, pads, and piston in order to detect instabilities in the system and thus predict potential squeal.

Nonlinearities arising from part-to-part interactions prove to be a frequent source of difficulty. Compared to the shape of real modes, a complex mode has a phase angle as its imaginary part, and therefore the points that make up the mode shape do not pass through their equilibrium simultaneously. The complete elimination of brake squeal still remains a somewhat illusive problem, as the system parameters need to be correlated and adjusted to make the FEM consistent with the measured experimental data.

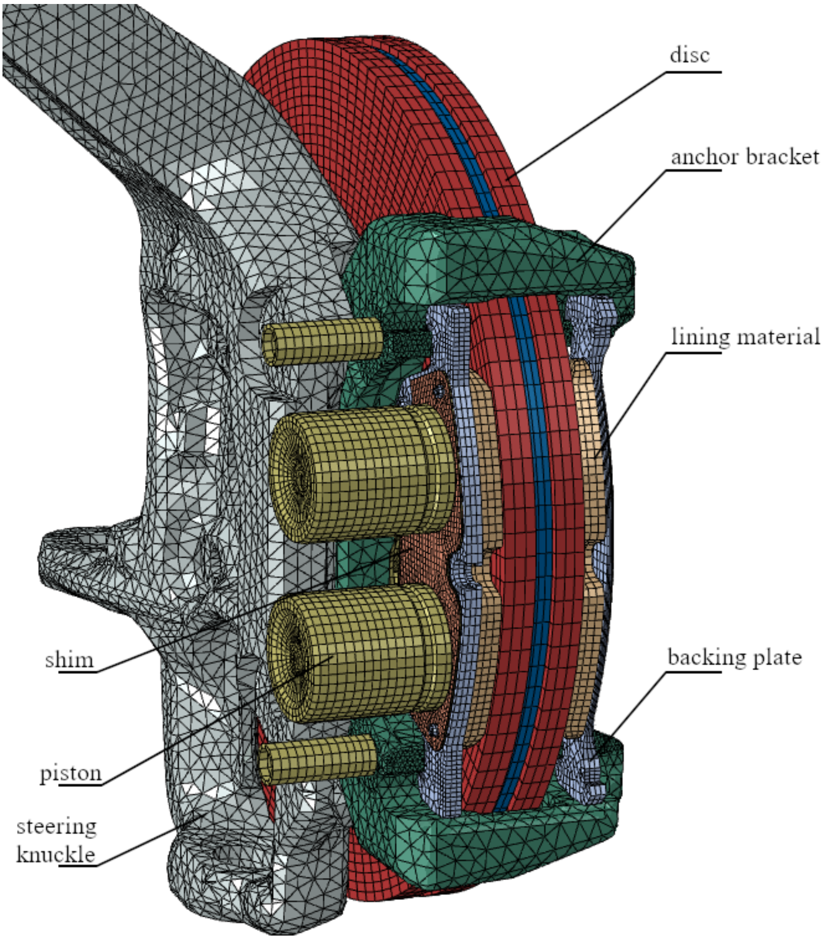

Fig. 1 FEM Disc brake assembly
Obr. 1 MKP Zostava brzdy

Material and methods

The CEA implementation in ABAQUS uses the subspace projection method. In this implementation, the response is based on the direct solution of the dynamical equations from the steady state projected into the subspace of undamped modes. The method is based on the idea that a number of modes of an undamped system that fall within the range of relevant excitation frequencies correctly reflect the forced steady-state vibrations. By projecting the equations of dynamic balance into the subspace of the selected modes, a system of complex equations is created. This system of equations is then solved for the modal amplitudes, which are then used to calculate nodal displacements, stresses, etc. It is an over-prediction method, which means that not all predicted modes will necessarily generate brake squeal under real operating conditions. The advantage of CEA over modal analysis performed in ABAQUS is the ability to account for friction and damping effects between parts.

For basic understanding of the, CEA the equation for a multi-degree finite element system with mass, stiffness and damping matrix has the form:

$$[M]\{\ddot{x}\} + [C]\{\dot{x}\} + [K]\{x\} = 0 \tag{1}$$

The homogeneous, second order matrix differential equation has a complementary solution that has the following shape:

$$\{u\} = \{\phi\}e^{\lambda t} \tag{2}$$

Solving and substituting we get the result in the form of the complex eigenvalue problem.

$$([M]\lambda^2 + [C]\lambda + [K])\{\phi\} = \{0\} \tag{3}$$

The eigenvalue pair for a given mode is complex. The eigenvalues for under damped systems always appear in complex conjugate pairs in the form:

$$\lambda_i = \sigma_{i\,+}\, j\omega_i \tag{4}$$

The σ denoting the real part of and ω the imaginary part. σ denoting the damping coefficient and ω the damped natural frequency which describe damped sinusoidal motion. The displacement of the nodes can be rewritten as periodic wave.

$$\{x_i\} = \{\phi\}e^{\sigma_i t}\cos\omega_i t \tag{5}$$

The effect of the damping material on the assembly of the brake system was evaluated by the FEM method in the CAE program ABAQUS. The assembly represents a brake system design common in commercial vehicles of today. The floating caliper disc brake together complete with a steering knuckle to which it is attached. Although the literature written so far indicates that the main source of vibration is mainly the brake disc and brake pads, the composition of the other components is more representative of the actual brake system in the car, although the effect of other parts is smaller due to the creation of their own shapes in some designs, which can introduce a large amount of damping into the system. The assembly of the brake system with a floating brake consists of the main parts: brake disc material, shims, caliper, caliper bracket, pistons, steering knuckle.

The aim of the experimental part is to correlate the assembly with the FEM model. The results are the natural frequencies and natural shapes using operation deflection shapes (ODS) scanned by a 3D laser measuring device. Excitation is performed by an automated impact hammer. For a relevant comparison, the mechanism of the hammer is fixed and automatically controlled, which guarantees an even constant blow to the same excitation point. The goal is to excite all relevant eigenshapes, as excitation at the nodal point of the deformation wave will not create a response, and it may happen that not all eigenfrequencies appear. A POLYTEC scanning station equipped with three laser sensors scanned a set of points of the brake system. Point by point was the system excited with the hammer during the scanning of the points. Subsequently, the system's own shape is assembled from the deformations of the individual points.

The equivalent of the previous measurement, but now as a discretized continuum solved on the basis of FEM, with the method of extracting complex shapes (complex eigenvalue analysis CEA). Certain procedures and simplifications were considered for a sufficient correlation of the CAD assembly with the experimental results, keeping in mind the computational possibilities. The material of the components is elastically isotropic, except for the lining material of the brake pads, which is transversely isotropic. The contact friction of the components is taken into account, and certain parts have been replaced with spring elements. The exact values of Young's modulus, stiffness, etc. were determined by testing from the basic values throughout the correlation of CEA eigenshapes with the experimental method. By correlating the output of the experimental part and the FEM model, the model represents the real brake with adequate accuracy, which means that subsequent design modifications on the correlated model will represent possible changes on the real brake as well. It is obvious that the adjustment in a representative FEM assembly is easier in terms of time and money than performing experimental measurements after each modification of the brake.

The surface friction contacts are formed in the first step of the simulation, and load is delivered to the piston surface in the form of pressure to cause the pads to grip the disc. In the second step, rotation is applied to the disc. The third step involves doing a modal analysis and extracting the eigenvalues and eigenvectors. In the last step, using the subspace-projection method, we extract the complex eigenvalues. This requires natural frequency beforehand, since this is the subspace to which the complex modes are mapped to. The simulation is then repeated for each pressure variant and for both friction coefficients.

RESULTS AND DISCUSSION

The findings demonstrate that the friction coefficient between the pads and the disc causes a change in the system's instability. As shown in **Fig. 3-5**, the friction between the pads and the disk significantly contributes to system instability. The numerous unstable modes are depicted on a stability plots, which also indicates the frequency at which the system instability occurs. The stability graphs exhibit symmetry between the positive and negative real components of the eigenvalue when damping is not considered. Higher friction coefficient values lead to additional unstable modes. This is most likely caused by a few closely spaced real modes combining into a complex one.

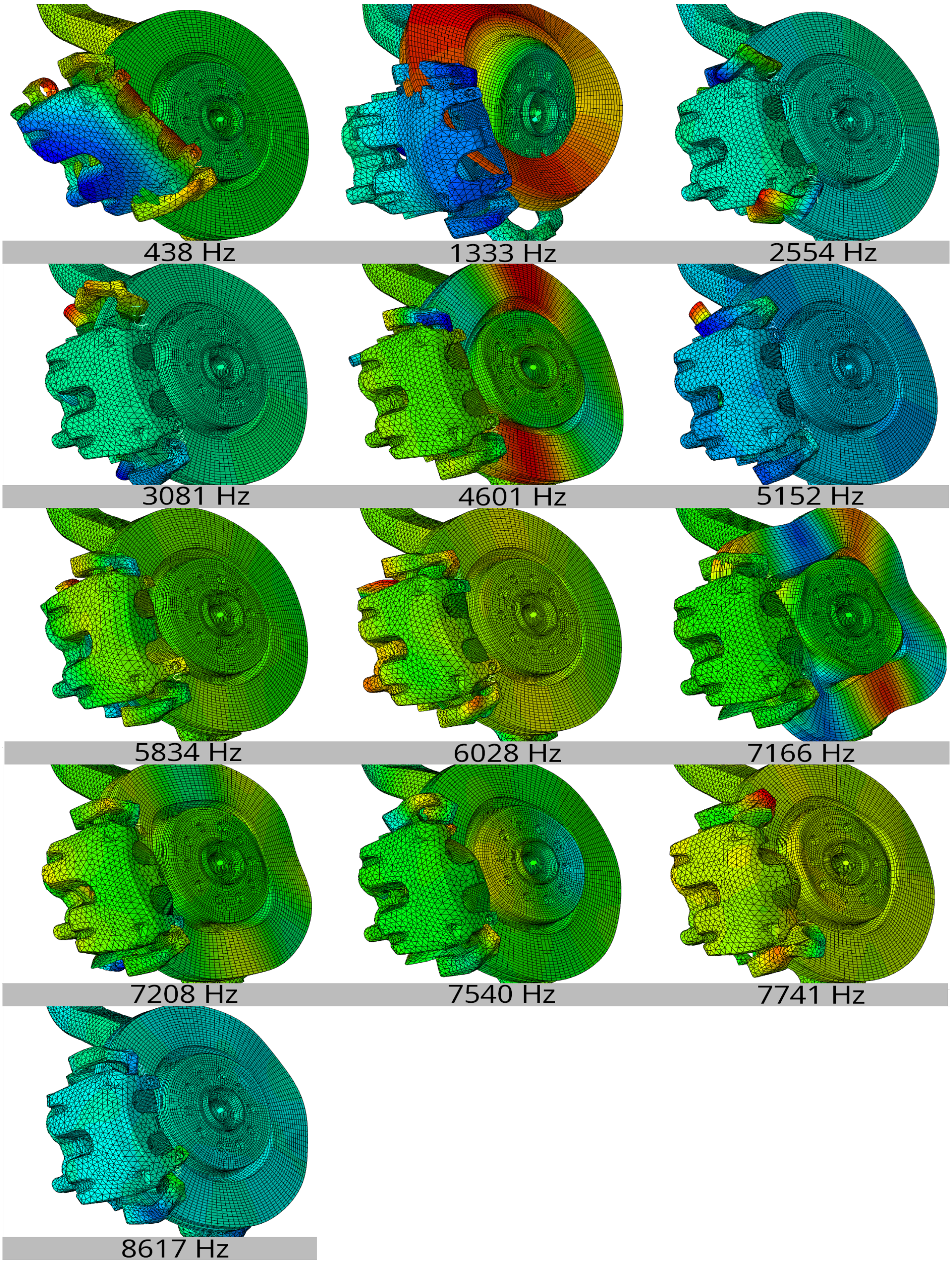

Fig. 2 Unstable complex mode shapes
Obr. 2 Nestabilné vlastné tvary

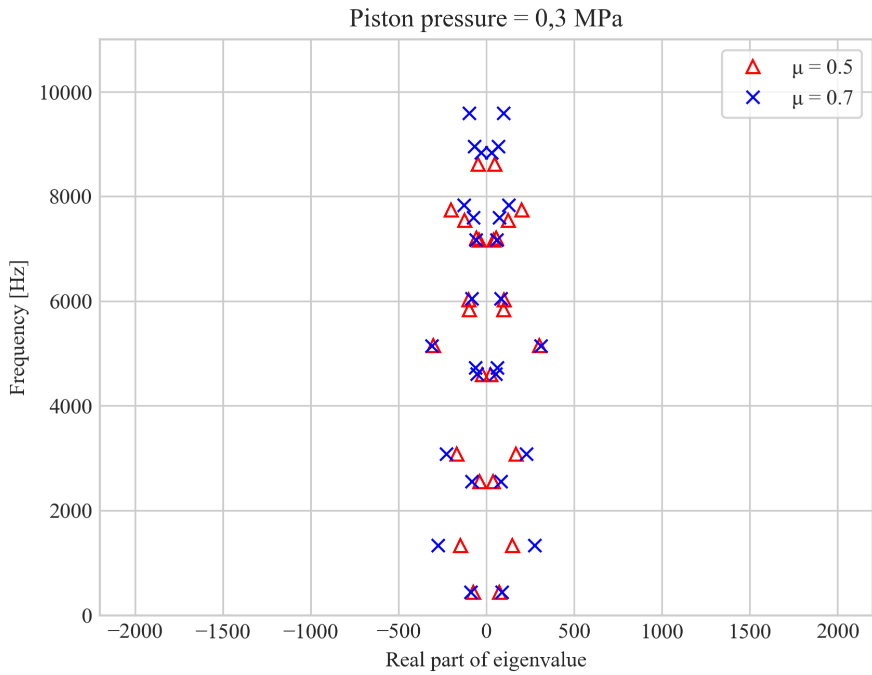

Fig. 3 Stability plot 0.3 MPa
Obr. 3 Stabilita 0.3 MPa

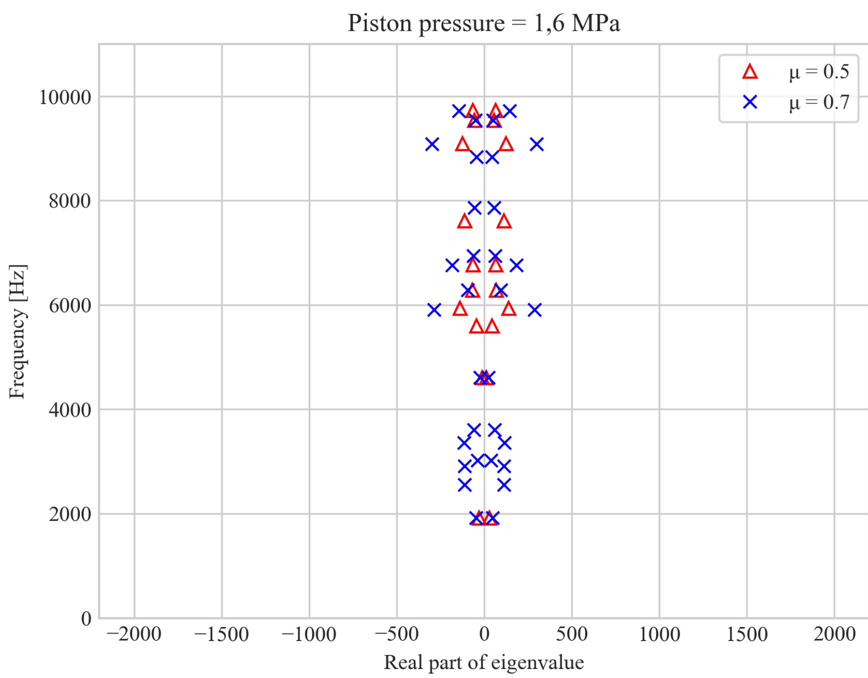

Fig. 4 Stability plot 1,6 MPa
Obr. 4 Stabilita 1,6 MPa

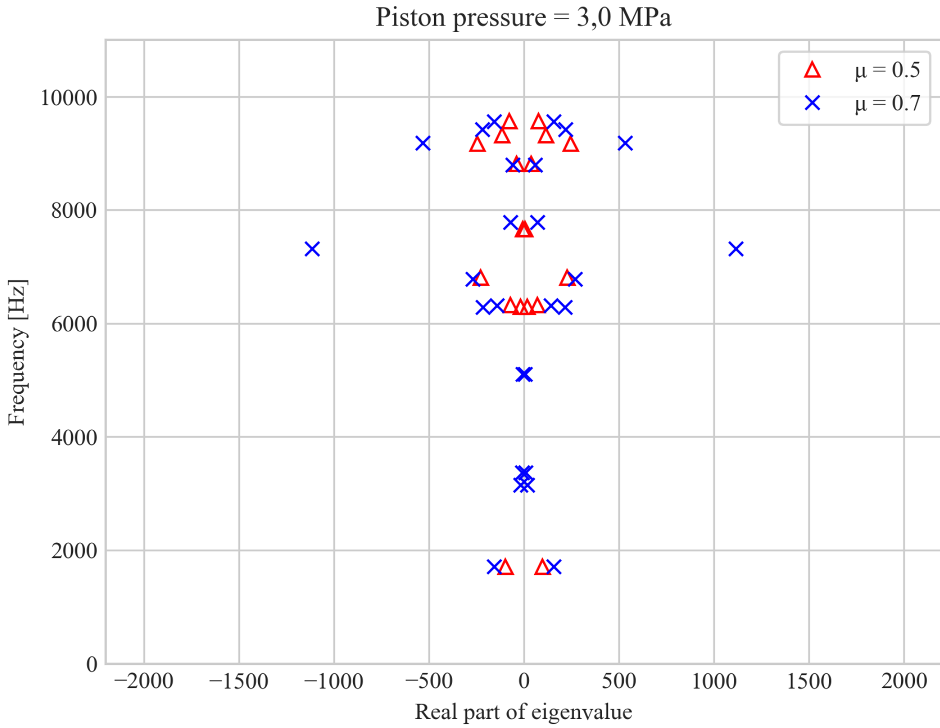

Fig. 5 Stability plot 3 MPa
Obr. 5 Stabilita 3 MPa

The system stability can be charted on a plot as frequency and the real part of the complex eigenvalue. The former being on ordinate and the latter as abscissa. From this stability chart the negative modes occurring at the negative side will be suppressed and modes on the right side are the unstable frequencies. As already mentioned not all of these unstable frequencies however will correspond to brake squeal in a real system because of the over-prediction of the CEA.

The **Fig. 3-5** show system stability plots for every combination of pressure and friction coefficient. Points in **Fig. 3-5** left side are stable modes, the amplitude of these the vibration will decline over time; any point on the chart's right side is an unstable mode, in which the magnitude will increase with time. Not all unstable modes lead to brake squeal. For example out of the 167 mode shapes found in the 0 to 10000 Hz spectrum during the modal analysis in the simulation with pressure = 0,3 MPa and μ = 0,5 it was only 12 of those modes **Fig. 2** had a potential for squeal according to the complex eigenvalue analysis.

CONCLUSION

High friction coefficient values, during braking between the disc rotor and the lining material of the brake pads, are a paramount factor for system instability to arise. In all cases, higher friction coefficient values gave rise to new unstable frequencies. These results agree with currently known research. If an unstable frequency was already present at a lower friction value, the subsequent increase did not cause it to shift on the frequency spectrum; however, the higher friction value was always associated with an increase in the real part of the eigenvalue. This research builds upon the work of (Liles et al. 1989) and explores the effects of complex modes on brake squeal while assuming mostly linear elastic material behavior. The brake assembly presented here consists of a disc, brake pads, lining material, and a piston. Incorporating a larger assembly would be suitable for future research to show how stability changes with more parts involved. Furthermore, additional insight could be gleaned by incorporating more non-linear system factors.

A complex eigenvalue stability analysis has been performed on a brake assembly system. The findings from the research presented to show how several parameters impact the probability of system instability. The following conclusions can be drawn. In summary:

- Unstable modes have been determined.
- Higher coefficient of friction gives rise to higher system instability.
- Higher pressure values give rise to higher system instability.

REFERENCES

DE SIMONE, MARCO A DOMENICO GUIDA, 2018. Modal Coupling in Presence of Dry Friction. Machines [online]. 2018, roč. 6, č. 1, s. 8. ISSN 2075-1702. Dostupné na: doi:10.3390/machines6010008

LAMARQUE, PV A C WILLIAMS, 1938. Brake squeak: the experiences of manufacturers and operators and some preliminary experiments. Institution of Automobile Engineers. 1938.

LILES, GREGORY D., 1989. Analysis of Disc Brake Squeal Using Finite Element Methods. V: SAE Noise and Vibration Conference and Exposition [online]. s. 891150 [cit. 9.6.2022]. Dostupné na: doi:10.4271/891150

LV, HONG-MING, LI-JUN ZHANG A ZHUO-PING YU, 2013. Influence of surface run-out on disc brake squeal. Journal of Vibroengineering. 2013, roč. 15, č. 2, s. 520–531. ISSN 1392-8716.

MILLS, H. R., 1938. Brake Squeak. B.m.: Institution of Automobile Engineers.

NOUBY, M, D MATHIVANAN A K SRINIVASAN, 2010. A combined approach of complex eigenvalue analysis and design of experiments (DOE) to study disc brake squeal. International Journal of Engineering, Science and Technology [online]. 2010, roč. 1, č. 1, s. 254–271. ISSN 2141-2839, 2141-2820. Dostupné na: doi:10.4314/ijest.v1i1.58084

NOUBY, M A K SRINIVASAN, 2011. Simulation of the structural modifications of a disc brake system to reduce brake squeal. Proceedings of the Institution of Mechanical Engineers, Part D: Journal of Automobile Engineering [online]. 2011, roč. 225, č. 5, s. 653–672. ISSN 0954-4070, 2041-2991. Dostupné na: doi:10.1177/2041299110394515

PARK, JOO SANG, JAE CHEOL LEE, SUNGSUN CHO A KYUWON YOON, 2012. Reduction of Brake Squeal Analyzed in Terms of Coupling Between In-Plane and Out-of-Plane Modes. SAE International Journal of Passenger Cars - Mechanical Systems [online]. 2012, roč. 5, č. 4, s. 1230–1243. ISSN 1946-4002. Dostupné na: doi:10.4271/2012-01-1828

Corresponding author:
Lukáš Hudec, e-mail: hudec.luk14@gmail.com

ACTA FACULTATIS TECHNICAE XXVII
ZVOLEN – SLOVAKIA 2022

APPLICATION OF AUGMENTED REALITY IN PUMP MAINTENANCE

APLIKOVANIE ROZŠÍRENEJ REALITY PRI ÚDRŽBE ČERPADLA

Mária Hrčková[1], Pavol Koleda[1], Martin Pinka[2]

[1] KVAT, FT,, TU Zvolen, Študentská 26, 960 53 Zvolen, Slovensko, hrckova@tuzvo.sk
[2] FT, TU Zvolen, Študentská 26, 960 53 Zvolen, Slovensko

ABSTRACT: In the article, we described the possibilities of practical use of augmented reality technology. We focused on the creation of 3D models for augmented reality and the creation of an application that will simplify the assembly and disassembly of the SPIRAM 150 pump. When creating it, we used a procedure that works with markers. We tested the finished application and described how to solve possible error conditions caused by the end user. The created application can be fully used in the process of production, sale, use and repair of the pump. Based on the implemented procedures, it is possible to extend the application to all series of SPIRAM pumps. It is also possible to modify the application so that it also works in other devices (augmented reality glasses), designed for augmented reality, or to respond to changes in hand position and hand gestures.

Key words: augmented reality, application, pump, assembly

ABSTRAKT: V článku sme popísali možnosti praktického využitia technológie rozšírenej reality. Zamerali sme sa na tvorbu 3D modelov pre rozšírenú realitu a tvorbu aplikácie, ktorá zjednoduší montáž a demontáž čerpadla SPIRAM 150. Pri jej vytváraní sme využili postup, ktorý pracuje s markermi. Hotovú aplikáciu sme testovali a popísali ako riešiť prípadné chybové stavy, spôsobené koncovým užívateľom. Vytvorenú aplikáciu je možné plnohodnotne využívať v procese výroby, predaja, využívania a opravy čerpadla. Na základe zrealizovaných postupov je možne aplikáciu rozšíriť na všetky série čerpadla SPIRAM. Rovnako je možné aplikáciu upraviť tak, aby fungovala aj v iných zariadeniach (okuliare pre rozšírenú realitu), určených pre rozšírenú realitu, prípadne aby reagovala na zmenu polohy rúk a gestá rúk.

Kľúčové slová: rozšírená realita, aplikácia, čerpadlo, montáž

INTRODUCTION

Augmented reality is a technology that supplements the real world with elements created virtually (3D model, information, animations, hologram or audio), thereby changing the perception of reality (Rebbani et al. 2021) (Valiauga 2020). Digital information does not replace the real environment, but overlaps it. The basic elements for devices working with augmented reality technology are hardware, software and application. For the proper functioning of augmented reality technology, the mutual cooperation of the mentioned elements is necessary (Chen 2019).

Augmented reality is used in various areas of industrial production, which ensure the support of the production process (Mendes et al. 2019). These are: product development, optimization of the working environment of machines, improvement of workplace ergonomics, layout planning, logistics, solutions and simulations of material and energy flows, material joining technologies, maintenance, assembly processes, quality control, but also presentations of products, designs, solutions, such as also the visualization of production premises, the layout of machines, the movement of handling equipment, training, tutorial programs.

By applying augmented reality, we will achieve the connection of workers from different departments with information in production, which is drawn from ongoing production processes. The result is increased quality and efficiency, reduced development and production time and costs, and increased worker flexibility (DePace et al. 2018). An accompanying phenomenon are greater requirements for the speed of education and professional training of workers, but also higher demands on devices used by augmented reality, for their accuracy and speed. A clear user interface is required for applications. The mentioned requirements also bring with them certain restrictions on the use of augmented reality, such as e.g. required quality of projection, calibration of the user‘s view, tracking and recognition of objects or high computing power of wearable devices (Horejší et al. 2020).

Among the expanded areas of use of augmented reality in Slovakia are:

Training of workers – based on ready-made applications, workers will receive accurate information about the product and its individual parts, and at the same time, based on a simulation that continuously provides the necessary information, they will learn how to assemble the product, or disassemble it in the maintenance process. The advantage is an increase in intuitive learning, the possibility of tracking performed actions, a reduction in error rates and high reliability (Kolla et al. 2020).

Component quality control – if the control worker has quick access to information about individual components through augmented reality, significant time savings occur.

Assembly – the idea of using digitized assembly instructions is one of the main tools of the currently introduced Industry 4.0 concept (Alcácer&Cruz Machado 2019). If the assembly simulation prepared in augmented reality (optimally also with information from sensors and with the results of immediate data analysis) is provided to the worker, ideally right in front of his eyes, then he has an overview of all the necessary actions and the sequence of their execution. At the same time, it also has various additional information available. In the case of using glasses for augmented reality, another advantage is free hands, with which he can work fluently (Border States 2021).

Maintenance – augmented reality brings an increase in its efficiency. Maintenance workers can use the augmented reality device to see potential failure points, allowing them to pinpoint the problem and identify faulty parts. They can then order them immediately. In a manufacturing company, even small service activities can be time-consuming due to the large amount of administration. Here, too, augmented reality can help, containing relevant data or the entire service history of the device.

In the post, we focused on the use of augmented reality in the process of staff training, communication with the customer, inspection of parts and in the process of assembly and disassembly of products, or their maintenance. The goal of our experiment was to create an application that simulates the assembly and disassembly process of a specific pump and at the same time allows viewing its individual parts in the form of 3D models.

MATERIAL AND METHODS

1. Object selection

The idea of producing a centrifugal slurry pump with one helical blade on an impeller arose based on the evaluation of the advantages that the mentioned type of impeller offers and also on the basis of a market survey, where a low number of manufacturers of pumps of a similar type was found (Figure 1). Screw pumps of the SPIRAM type are used in wastewater treatment, in the food and processing industry.

Figure 1 Screw pump SPIRAM by PraktikPump
Obrázok 1 Skrutkovicové čerpadlo SPIRAM firmy PraktikPump

The SPIRAM 150 pump was chosen to create an augmented reality application for several reasons. Achieving an increase in the clarity and comprehensibility of the production of pump parts during the production process, which we will ensure if, as a supplement to the drawings, 3D models of individual parts are also available in augmented reality. Especially in the design of castings, individual parts of the pump, presented in augmented reality, will make it possible to find the thin walls of the casting, which will enable the correct determination of the casting technology. Errors often occurred during pump assembly, which caused a time mismatch with customer requirements. There have also been cases of ordering the wrong pump part during its repair. Last but not least, the goal was to simplify and make working with the pump itself and its individual parts more transparent, as well as to interest potential customers with a simple and vivid display of the actual assembly and disassembly of the pump.

2. Choosing an environment to create an application

Due to the experience of working in the Creo Parametric program from PTC, we used this CAD program to create 3D models, in which the work is intuitive and parametric modeling creates suitable prerequisites for very easy modification of models for other dimensional sets of individual pump series.

The PTC company also has at its disposal a powerful program for working with augmented reality, Vuforia Studio, primarily intended for industry, and therefore this tool became our first choice when creating an application in augmented reality. It allows to recognize images, objects and spaces and realize their interaction with the real world.

Given that we were creating the application for a handheld device – a mobile phone and for digital glasses, we chose the Unity programming platform. Unity is a popular and useful platform for creating high-end augmented reality applications. We installed Vuforia Studio in Unity.

RESULTS AND DISCUSSION

1. Creation of a CAD model

When creating the 3D model of the SPIRAM 150 pump, we were based on the input parameters: throughput (suction diameter) and displacement (the height to which the pump should push the transported medium). We calculated these data in the ANSYS program, which, based on the input information: pump size, revolutions, displacement, determines exactly the internal shape and geometry of the blade of individual sizes of the SPIRAM pump. Figure 2 shows the output from the ANSYS program, based on which the pump parts themselves were modeled. Through the simulation, we will determine the pitch of the impeller helix and the internal shape of the pump body itself.

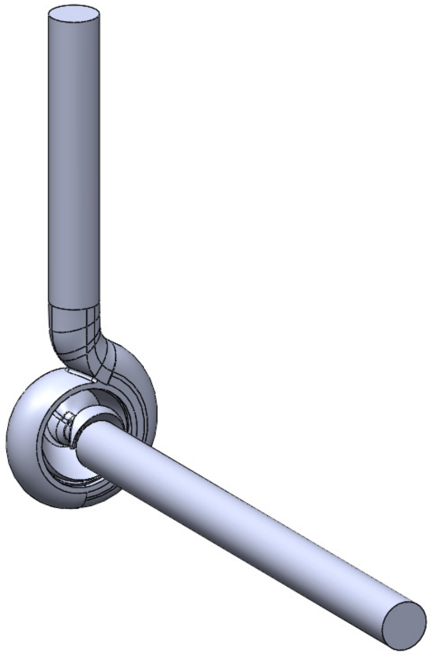

Figure 2 The geometry of the SPIRAM 150 pump
Obrázok 2 Geometria čerpadla SPIRAM 150

Based on the speed and power of the pump, we determined the dimensions of the bearings and the shaft according to the tables. The dimensions must be in accordance with the dimensions of the bearing housing. Subsequently, we designed the individual parts of the pump in the Creo Parametric program. In Figure 3 we see the suction flange of the SPIRAM 150 pump.

The other parts of the pump were also modeled analogously: the front and rear disc, the specific impeller and its carrier, the pump body itself, the shaft that transmits the torque from the motor to the impeller. Standardized parts such as bearings, screws, motor were requested from manufacturers in the form of 3D models. The assembly of the SPIRAM 150 pump was created from all the parts through movement and fixed links. The said assembly was the basis for the creation of a simulation of the assembly of the pump in augmented reality.

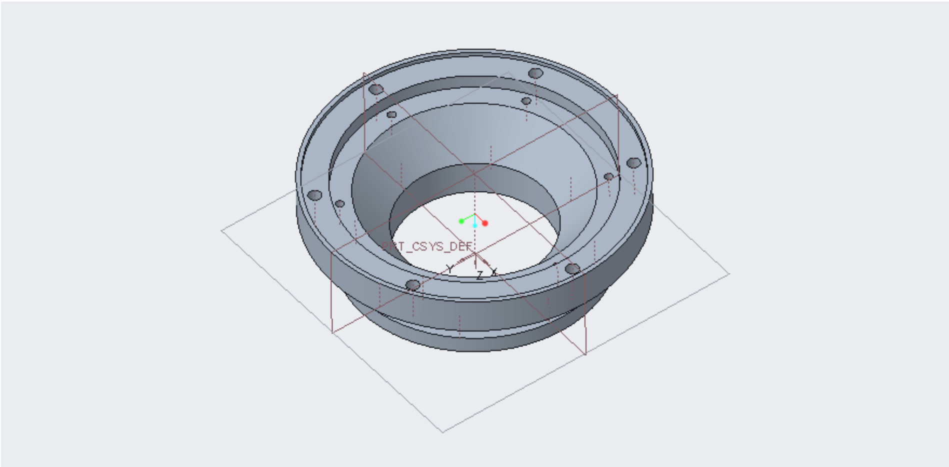

Figure 3 Design of the suction flange of the SPIRAM 150 pump
Obrázok 3 Návrh sacej príruby čerpadla SPIRAM 150

2. Creation of an application for viewing pump parts

We used Unity (Figure 4) and Vuforia programs to create an augmented reality application.

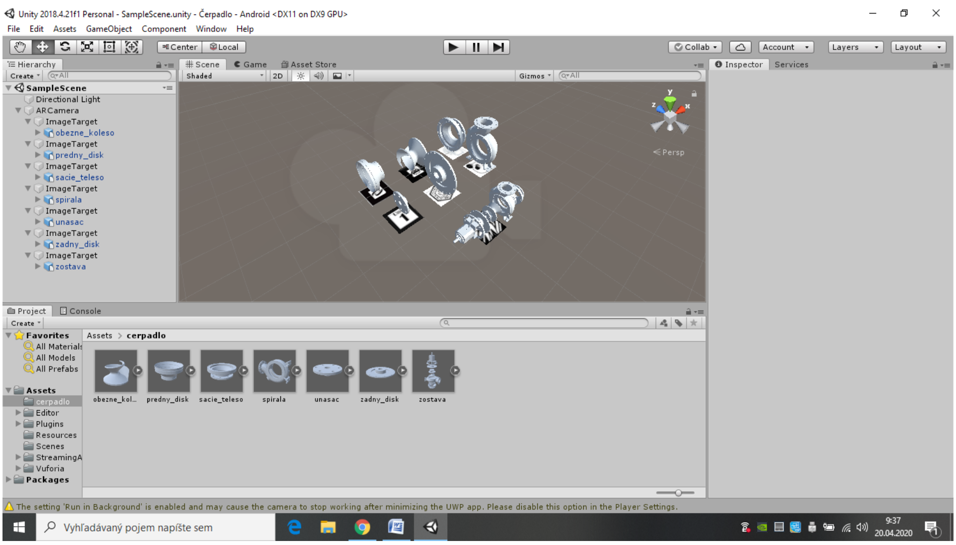

Figure 4 Unity workspace
Obrázok 4 Pracovný priestor Unity

In the Unity program, we set up the camera for augmented reality and defined the objects with which we will work. We worked with augmented reality based on markers

(Novak-Marcinčin et al. 2012). After creating a camera for augmented reality, it was necessary to insert a basic marker (an image to which we will associate a specific part of the pump). We created a database of our own markers (Figure 5). Images that met the basic conditions were used as markers: simplicity, .jpg format and size below 2 MB. The images used cannot be similar or repeated. We checked their suitability directly in the Unity program.

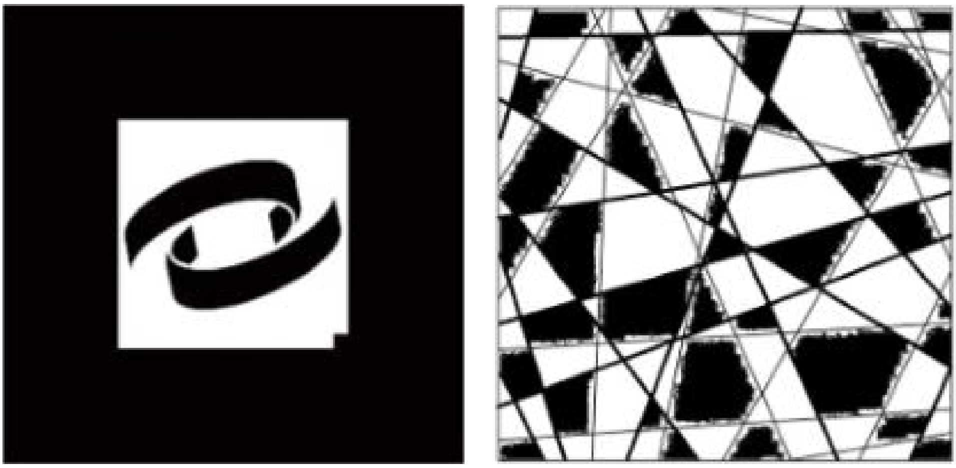

Figure 5 Selected markers for the SPIRAM 150 series
Obrázok 5 Vybrané markery pre sériu SPIRAM 150

The models that we want to work with in augmented reality and that we prepared in Creo Parametric were gradually uploaded to the Unity program. We assigned a unique marker from the database to each model. The position of the 3D model had to be in the space above the marker (Figure 6).

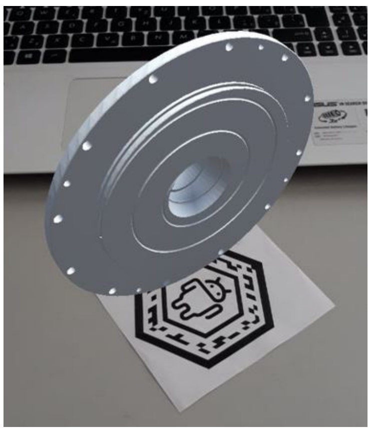

Figure 6 Placing the model above the marker

Obrázok 6 Umiestnenie modelu nad marker

3. Creation of an application for a demonstration of pump assembly

The application was created in order to facilitate the maintenance and assembly of the SPIRAM 150 pump. To create a sequence of individual steps for assembling the pump, a program from the group of CREO programs from the PTC company Creo Illustrate (Figure 7) was used. In this program, we set individual steps for mounting or dismounting the pump.

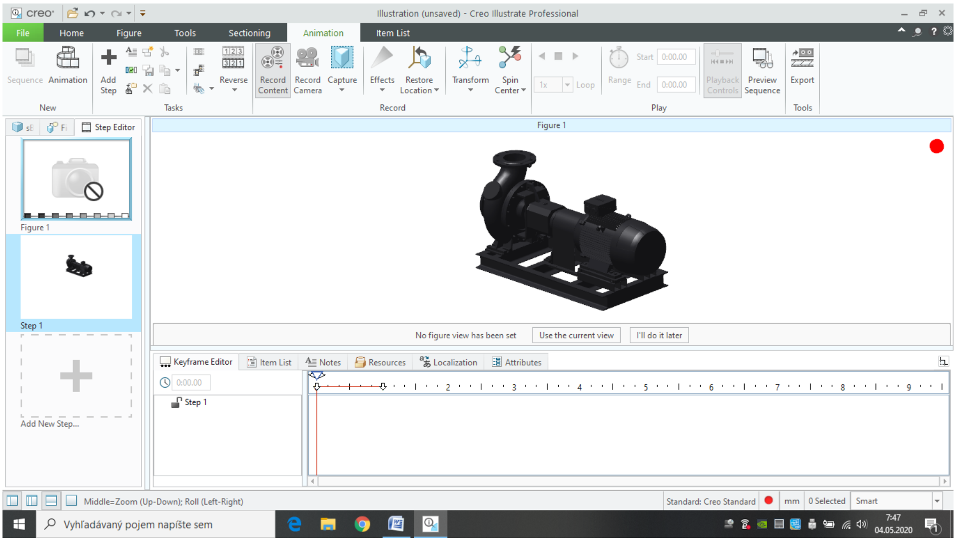

Figure 7 Open assembly of the SPIRAM 150 pump in Creo Illustrate
Obrázok 7 Otvorená zostava čerpadla SPIRAM 150 v Creo Illustrate

When the pump assembly procedure was finished, we saved the pump assembly in .pzv format, which is intended for augmented reality, which will create a simulation of the pump disassembly and assembly based on the designed procedure. We used the Vuforia Studio program to create the pump folding animation (Figure 8).

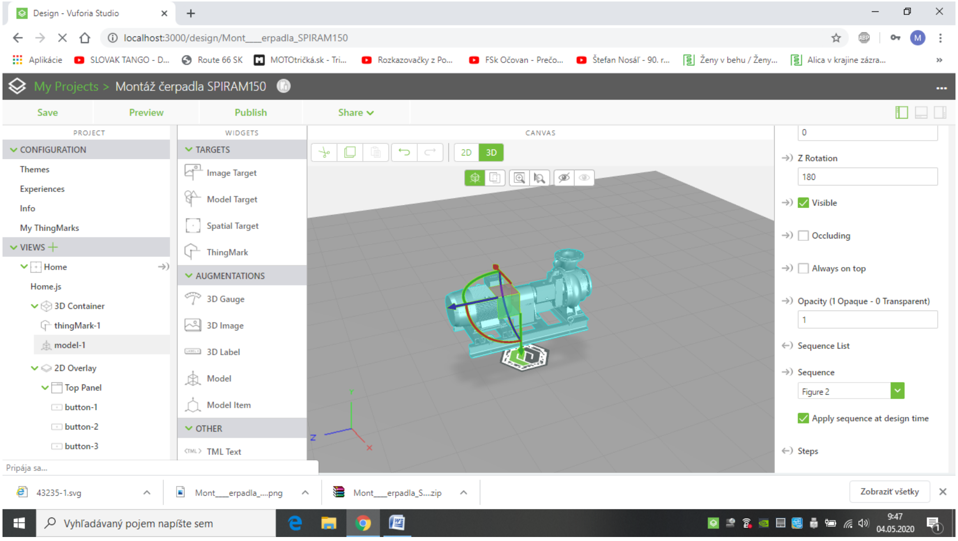

Figure 8 Vuforia Studio workspace
Obrázok 8 Pracovný priestor Vuforia Studio

After defining the basic marker and setting the assembly sequence, which ensured the use of the created movement study, we proceeded to create a user interface for ordinary users of the application, who will be able to choose whether they want to assemble or disassemble the pump, as well as whether they want to run the entire procedure continuously or step by step (Figure 9).

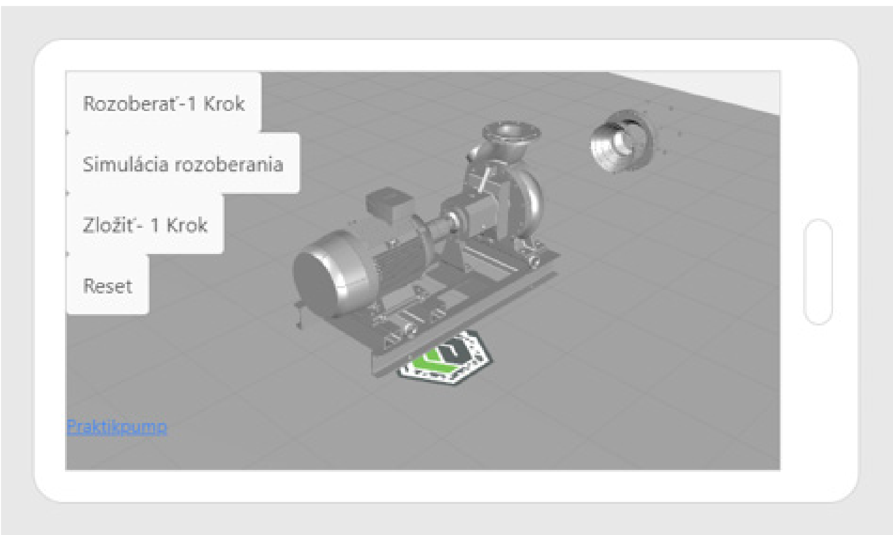

Figure 9 User interface
Obrázok 9 Používateľské rozhranie

4. Test of application

We installed the created application on a device with the Android operating system. First, we checked the 3D models of the individual parts of the pump and their location relative to the markers. The assignment of models to individual markers was fast. In two cases, when rotating the marker, the model moved incorrectly, which was caused by the insufficient scanning of the marker (the marker was not completely captured by the camera). By reloading it, the flaws were removed. The application downloaded the necessary data from the Cloud and, after reading the QR code, drew the pump on the device's display (Figure 10). In other tests, we monitored the marker, its shooting, position and distance. We found no errors.

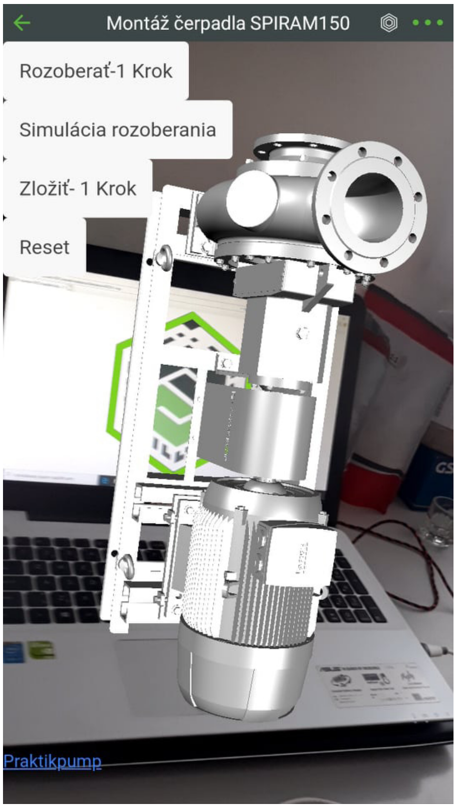

Figure 10 The workspace of the created application for AR
Obrázok 10 Pracovný priestor vytvorenej aplikácie pre AR

CONCLUSION

The result of the design is an application that shows us 3D models of individual parts of the SPIRAM 150 pump and simulates the pump assembly and disassembly procedure.

The creation of the application requires knowledge of CAD modeling, as well as the basic principles of the operation of augmented reality. When creating the application, we used products from PTC (Creo and Vuforia Studio) and Unity Technologies (Unity Personal). The finished application found its use in the maintenance of the mentioned pump. In the next stage, it is assumed, based on the requirements of practice, to supplement the application so that it includes all series of SPIRAM pumps. A significant benefit would also be its modification in the sense that it responds to different hand positions and gestures.

ACKNOWLEDGMENT

The article was developed within the framework of the VEGA 1/0791/21 project: Research of non-contact method of analysis of small and dust particles arising in the production process with a prediction of negative effects of dust particles.

The article was developed within the framework of the KEGA 006STU-4/2021 project: Progressive form of interdisciplinary education and support for the development of the study of vocational subjects in the university environment.

REFERENCES

ALCÁCER, V.; CRUZ-MACHADO, V. 2019. Scanning the industry 4.0: A literature review on technologies for manufacturing systems, Engineering Science and Technology, International Journal, vol. 22, no. 3, 2019, pp. 899–919. https://doi.org/10.1016/j.jestch.2019.01.006.

BORDER STATES 2021. Exciting Industrial Applications for Augmented Reality (AR) in 2021 and Beyond [online, 11.8.2022]. https://solutions.borderstates.com/benefits-of-industrial-augmented-reality/.

DE PACE, F.; MANURI, F.; SANNA, A. 2018. Augmented Reality in Industry 4.0. American Journal of Computer Science and Information Technology, vol. 6, no. 1, 2018, pp. 0–7. https://doi.org: 10.21767/2349- 3917.100017.

HOŘEJŠÍ, P.; NOVIKOV, K.; ŠIMON, M. 2020. A Smart Factory in a Smart City: Virtual and Augmented Reality in a Smart Assembly Line. in IEEE Access vol. 8, 2020, pp. 94330–94340. DOI:10.1109/ACCESS.2020.2994650.

CHEN, R. 2019. Augemented reality (AR): How does it work?, [online, 11.8.2022]. https://www.constructdigital.com/insight/how-does-augmented-reality-ar-work.

KOLLA, S.S.V.K.; SANCHEZ A.; MINOUFEKR M.; PLAPPER P. 2020. Augmented Reality in Manual Assembly Processes. Augmented Reality in Manual Assembly Processes. 9 Internaonal Conference on Mass Customizaon and Personalizaon – Community of Europe (MCP - CE 2020) pp: 121–128.

MENDES, M.; ALMEIDA, J.; MOHAMED, H.; GIOT, R. 2019. Projected Augmented Reality Intelligent Model of a City Area with Path Optimization, Algorithms, vol. 12, no. 7, 2019, p. 140. https://doi.org: 10.3390/a12070140.

NOVÁK-MARCINČIN, J.; BARNA, J.; JANÁK, M. 2012. Využívanie Open Source nástrojov pri aplikácii rozšírenej reality v technológii montáže (1). ATP Journal Vol: 2, 2012. pp: 42-45.

REBBANI, Z.; AZOUGAGH, D.; BAHATTI, L.; BOUATTANE, O. 2021. Definitions and applications of augmented/virtual reality: International Journal of Emerging Trends in Engineering Research, Volume 9. No. 3, 2021, https://doi.org/10.30534/ijeter/2021/21932021.

VALIAUGA, P. 2020. Ako rozšírená a zmiešaná realita zapadajú do priemyslu 4.0, ATP Journal, [online, navštívené 12.8.2022]. Dostupné na: https://www.atpjournal.sk/rubriky/prehladove-clanky/ako-rozsirena-azmiesana-realita-zapadaju-dopriemyslu4.0.html?page_id=31011.

Corresponding author:
Ing. Mária Hrčková, PhD., tel.: +421 45 5206 565, e-mail: hrckova@tuzvo.sk